THE ROLE OF PGE$_2$ BIOSYNTHESIS AND METABOLISM IN LIVER INJURY

AND LIVER CANCER

AN ABSTRACT

SUBMITTED ON THE TWENTY DAY OF NOVEMBER 2015

TO THE GRADUATE PROGRAM IN BIOMEDICAL SCIENCES

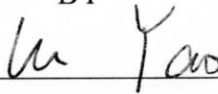IN PARTIAL FULFILLMENT OF THE REQUIREMENTS

OF THE SCHOOL OF MEDICINE

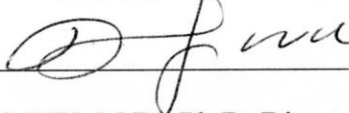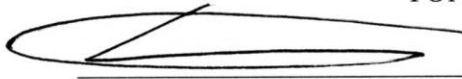OF TULANE UNIVERSITY

FOR THE DEGREE

OF

DOCTOR OF PHILOSOPHY

BY

_____

LU YAO

APPROVED:

_____

TONG WU, M.D., Ph.D. Director

_____

ERIK K FLEMINGTON, Ph.D.

_____

ZACHARY PURSELL, Ph.D.

_____

GILBERT F. MORRIS, Ph.D.

_____

ZONGBING YOU, Ph.D.

ABSTRACT

PGE$_2$ plays an important role in liver inflammation and carcinogenesis. Its metabolism is regulated by a cascade of reactions catalyzed by enzymes including COX-1/2, mPGES-1/2, 15-PGDH. Among these regulators, mPGES-1 is a cytokine-inducible enzyme mainly responsible for catalyzing terminal synthesis of PGE$_2$, 15-PGDH catalyzes the oxidation of PGE$_2$ to 15-keto-PGE$_2$. In this context, we exogenously expressed mPGES-1 or 15-PGDH genes in mice hepatocytes to constitute a physiological condition ideal for evaluating PGE$_2$ and its metabolites function in liver pathogenesis.

In the first part, we developed transgenic mice with targeted expression of mPGES-1 in the liver and assessed the response of the transgenic mice to Fas-induced hepatocyte apoptosis and acute liver injury. Compared to wild type mice, the mPGES-1 Tg mice showed less liver hemorrhage, lower serum alanine transaminase and aspartate transaminase levels, less hepatic necrosis/apoptosis, and lower levels of caspase activation after intraperitoneal injection of the anti-Fas antibody Jo2. Western blotting analyses revealed increased expression and activation of the serine/threonine kinase Akt and associated anti-apoptotic molecules in the liver tissues of Jo2-treated mPGES-1 Tg mice. Pretreatment with the mPGES-1 inhibitor (MF63) or the Akt inhibitor (Akt inhibitor V) restored the susceptibility of the mPGES-1 Tg mice to Fas-induced liver injury. Our findings provide novel evidence that mPGES-1 prevents Fas-induced liver

injury through activation of Akt and related signaling. This finding is consistent with previous reports of the anti-apoptotic and pro-proliferative role of PGE$_2$. Our results suggest that induction of mPGES-1 or treatment with PGE$_2$ may represent a potential therapeutic strategy for the prevention and treatment of Fas-associated liver injuries.

In the second part, we generated transgenic mice with targeted expression of 15-PGDH in the liver and the animals were subjected to LPS/GalN-induced acute liver inflammation and injury. Compared to the wild type mice, the 15-PGDH Tg mice showed lower levels of alanine aminotransferase and aspartate aminotransferase, less liver tissue damage, less hepatic apoptosis/necrosis, less macrophage activation, and lower inflammatory cytokine production. In Kupffer cell cultures, treatment with 15-keto-PGE$_2$ or the conditioned medium (CM) from 15-PGDH Tg hepatocyes inhibited LPS-induced cytokine production. Both 15-keto-PGE$_2$ and the CM from 15-PGDH Tg hepatocyes also up-regulated the expression of PPAR-γ downstream genes in Kupffer cells. In cultured hepatocytes, 15-keto-PGE$_2$ treatment or 15-PGDH overexpression did not influence TNF-α-induced hepatocyte apoptosis. These findings suggest that 15-PGDH protects against LPS/GalN-induced liver injury and the effect is mediated via 15-keto-PGE2, which activates PPAR-γ in Kupffer cells and thus inhibits their ability to produce inflammatory cytokines. Accordingly, we observed that the PPAR-γ antagonist, GW9662, reversed the effect of 15-keto-PGE$_2$ in Kupffer cell in vitro and restored the susceptibility of 15-PGDH Tg mice to LPS/GalN-induced acute liver injury in vivo. Our findings not only support the pro-inflammatory role of PGE$_2$, but also reveal a novel anti-inflammatory role of 15-keto-PGE$_2$. The data suggest that induction of 15-PGDH

expression or utilization of a 15-keto-PGE$_2$ analog may be therapeutic for treatment of endotoxin-associated liver inflammation/injury.

Consistent with a pro-carcinogenic role for PGE$_2$, overexpression mPGES-1 enhances growth of either HCC or cholangiocarcinoma cells, while overexpression 15-PGDH inhibits tumor cell growth in vitro. In the third part, we use a pharmacological method to induce 15-PGDH in cholangiocarcinoma tumor cells to inhibit PGE$_2$ production. Our results indicated that treatment of human cholangiocarcinoma cells (CCLP1 and TFK-1) with ω-3 PUFA (DHA) or transfection of these cells with the Fat-1 gene (encoding Caenorhabditis elegans desaturase which converts ω-6 PUFA to ω-3 PUFA) significantly increased 15-PGDH protein level in cholangiocarcinoma cell lines. Human cholangiocarcinoma cells treated with DHA or transfected with a Fat-1 expression vector showed reduction of miRNA26a and miRNA26b (both miRNAs target 15-PGDH mRNA thus inhibiting 15-PGDH translation). Consistent with these findings, we observed that overexpression of miR26a or miR26b decreased 15-PGDH protein, reversed ω-3 PUFA-induced accumulation of 15-PGDH protein, and prevented ω-3 PUFA-induced inhibition of cholangiocarcinoma cell growth. Knockdown of 15-PGDH also attenuated ω-3 PUFA-induced inhibition of tumor cell growth. We observed that ω-3 PUFA suppressed miRNA26a and miRNA26b by inhibiting c-myc, a transcription factor that co-regulates a gene cluster comprised of miR-26a/b and carboxy-terminal domain RNA polymerase II polypeptide A small phosphatases (CTDSPs). Accordingly, overexpression of c-myc enhanced the expression of miRNA26a/b and prevented ω-3 PUFA-induced inhibition of tumor cell growth. Taken together, our results support a

pro-tumorigenic role for PGE$_2$, and suggest induction of 15-PGDH as potential way for

the prevention and treatment of human cholangiocarcinoma.

THE ROLE OF PGE$_2$ BIOSYNTHESIS AND METABOLISM IN LIVER INJURY

AND LIVER CANCER

A DISSERTATION

SUBMITTED ON THE TWENTY DAY OF NOVEMBER 2015

TO THE GRADUATE PROGRAM IN BIOMEDICAL SCIENCES

IN PARTIAL FULFILLMENT OF THE REQUIREMENTS
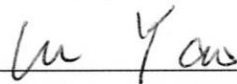
OF THE SCHOOL OF MEDICINE

OF TULANE UNIVERSITY

FOR THE DEGREE
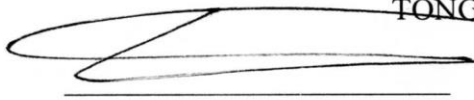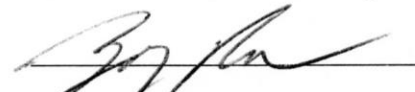
OF

DOCTOR OF PHILOSOPHY

BY

_____

LU YAO

APPROVED:

_____

TONG WU, M.D., Ph.D. Director

_____
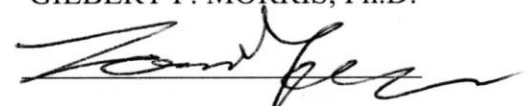ERIK K FLEMINGTON, Ph.D.

_____
GILBERT F. MORRIS, Ph.D.

_____
ZACHARY PURSELL, Ph.D.

_____
ZONGBING YOU, Ph.D.

ACKNOWLEDGEMENT

I would like to thank my mentor Dr. Tong Wu and Dr. Chang Han. They lead me into professional world of biomedical research and provide a systematic training in liver disease study. Under their instruction and encouragement, I am making progress and finally complete my Ph.D. study.

I would like to thank my committee member Dr. Erik Flemington, Dr. Gilbert Morris, Dr. Zongbing You and Dr. Zachary Pursell for their precious time and insightful comments.

I would like to thank my previous and current colleagues Dr. Dongdong Lu, Dr. Weina Chen, Dr. Jinqiang Zhang, Dr. Kyoungsub Song, Dr.Ximena V.Qadir, Dr. Lu Lu and Dr. Hanqing Zhu, Hyunjoo Kwon and Nate Ungerleider. Their enthusiastic and critical thinking make the bench work more interesting and enjoyed.

My special thanks go to my girlfriend. She always rescues me from depression, comforts me when I am sick and helps me establish a more meaningful life attitude.

Last, I would show my deeply appreciation for my parent, for their forever love, for their unconditional endorsement, for their always being there. Without their sacrifice, I won't make this long journey. I take this work as the gift to them.

TABLE OF CONTENT

LIST OF FIGURES

CHAPTER I INTRODUCTION

1 General overview of Prostaglandin E$_2$

PGE_2 is the physiologically active lipid derived enzymatically from fatty acids containing 20 carbon atoms, including a 5-carbon ring. PGE_2 is well noted as the bioactive mediator that is strongly associated with inflammation and carcinogenesis. PGE_2 carries out its function via binding to its receptor (EP1-4, members of GPCR family). Upon PGE_2 binding, EP receptors are coupled to Gα proteins (containing stimulatory Gs or inhibitory Gi subunits) to modulate the levels of Ca2+, cAMP and inositol phosphate, and activate downstream signaling pathways. These pathways potently regulate diverse biological effects, including cell proliferation, apoptosis, angiogenesis, inflammation and immune surveillance in different cell types within a wide range of tissues [1]. EP receptors are ubiquitously expressed [2]. EP3 and EP4 represent high-affinity receptors, whereas EP1 and EP2 require significantly higher concentrations of PGE_2 for effective signaling. EP2 and EP4 are coupled to Gs subunits and thought to signal in a largely cAMP- and PI3K-dependent fashion [3]. Furthermore, both EP2 and EP4 have been shown to activate the GSK3/β-catenin pathway [4]. In contrast to EP2 and EP4, low-affinity EP1 and high affinity EP3 do not couple to Gs, and therefore lack cAMP-activating functions. Most of the splice variants of EP3 represent Gi-coupled

PGE_2 receptors that inhibit adenylate cyclase [5], while signaling via EP1 involves calcium release [5].

The synthesis of PGE_2 is regulated by an array of sequential reactions, which starts from liberating free fatty acids (Arachidonic acid, AA) from membrane phospholipids. $cPLA_{2\alpha}$ is the best characterized phospholipase isoform catalyzing this step. $cPLA_{2\alpha}$ activity is regulated by Ca2+ and phosphorylation by MAPK [6]. AA derived from membrane lipids is oxidized by cyclooxygenase (COX) into the relatively unstable metabolite PGH_2. Two isoforms of COX are responsible for catalyzing this step. COX-1 is expressed in most tissues. In contrast, constitutive COX-2 expression is restricted to the kidney and central nervous system, but highly inducible by pro-inflammatory stimuli in many other tissues [7, 8]. Unstable PGH_2 is rapidly converted into prostanoids by various terminal synthases. Three distinct synthases contribute to PGE_2 synthesis, including mPGES-1, mPGES-2, and cPGES [9]. mPGES-2 and cPGES are constitutively expressed and are functionally coupled with COX-1 to maintain basal levels of PGE_2. On the other hand, mPGES-1 is a cytokine-inducible enzyme similar to COX-2 and is induced concomitantly with COX-2 to boost PGE_2 production [10]. The metabolic turnover of PGE_2 is regulated by 15-PGDH, which catalyzes the oxidation of the 15(S)-hydroxyl group of PGE_2, converting PGE_2 to its oxidized product 15-keto-PGE_2. While 15-keto-PGE_2 has long been viewed as a biologically inactive metabolite of PGE_2, recent studies show that 15-keto-PGE_2 actually functions as an endogenous ligand for PPAR-γ [11, 12]. In a mouse model of CFTR-deficiency, regulation of PPAR-γ by 15-keto-PGE_2 is implicated in the pathogenesis of cystic fibrosis [13]. In mouse fibroblasts, 15-keto-PGE_2 activates PPAR-γ and thereby promotes adipocyte maturation

[14]. In liver tumor cells, 15-keto-PGE$_2$ has been found to activate PPAR-γ and regulate its downstream genes.

1.1 The role of PGE$_2$ in inflammation and tissue homeostasis

The influence of PGE$_2$ on inflammation depends on pathological context. PGE$_2$ plays a critical role in the establishment of acute inflammation, while promoting resolution of chronic inflammation, leading to tissue regeneration and the return to homeostasis [1].

PGE$_2$ initiates vasodilation and facilitates immune cell recruitment. On the other hand, PGE$_2$ increases pain by acting on sensory nerves and promoting pyrogenic effects by acting in the preoptic area [15]. Recently, PGE$_2$ has also been reported to promote activation of Th17 cells, which accounts for the production of the pro-inflammatory IL-17 family cytokines. IL-17 mediates monocyte and neutrophil recruitment, contributing to the development of inflammatory diseases like collagen-induced arthritis and inflammatory bowel disease in mice [16, 17].

In contrast, PGE$_2$ is also a key component of anti-inflammatory processes and mediates immunosuppressive activities by inhibiting production of specific cytokines/chemokines and their cognate receptors in immune, stromal and epithelial cells. In monocytes and dendritic cells, PGE$_2$ inhibits production of CCL19 which plays a key role in attracting native T cells [18]. In T cells, PGE$_2$ inhibits synthesis of IL2 and its receptor, and promotes a change in the immune response from a Th1 to a Th2 response (Th1 response promotes tissue damage while Th2 response generally promotes scarring)

[2]. In addition, PGE$_2$ suppresses the cytotoxicity and cytokine production of natural killer cells via EP4 signaling [19]. The polarization of tumor-associated macrophages (TAMs) towards tumor-promoting M2 macrophages is also regulated by PGE$_2$ [20].

PGE$_2$ not only inhibits harmful inflammation, but also promotes tissue repair. PGE$_2$ enhances VEGF expression in lung and stomach fibroblasts and promotes angiogenesis. The PGE$_2$-EP4 axis has been shown to mediate such effects and control the differentiation of endothelial cells via the activation of MAPK [21]. PGE$_2$ also inhibits myofibroblast differentiation and collagen deposition during tissue fibrosis of lung, skin and liver via EP1/EP3 signaling [22], and generally promotes tissue regeneration. PGE$_2$ activates several key pro-survival pathways, including PI3K/Akt, MAPK and JNK pathways, via transactivation of EGFR [23]. Inhibiting PGE$_2$ production with a COX-2 inhibitor delays tissue repair in the liver, lung and colon after injury [24]. PGE$_2$ facilitates maintenance and expansion of several types of tissue stem cells, including hematopoietic and colon stem cells, by enhancing Wnt signaling [25]. Administration of PGE$_2$ or its more stable analog dmPGE$_2$ enhanced engraftment of murine bone marrow cells and stimulated regeneration of intestinal crypts after irradiation [26]. Moreover, enhancing PGE$_2$ production by inhibition of 15-PGDH potentiates tissue regeneration in multiple organs in mice [25].

1.2 The role of PGE$_2$ in carcinogenesis

In the context of cancer, PGE$_2$ is generally recognized to promote tumor progression. A broad array of clinical data and experimental studies demonstrates a pro-

carcinogenic role for PGE_2. Elevated levels of COX-2 and PGE_2 are detected in the majority of colorectal carcinomas and in a subset of adenomas [27, 28]. Epidemiological studies show that treatment with a COX-2-selective inhibitor NSAID (like aspirin) at low doses is associated with a 50 percent reduction in the risk for colon and rectal cancers [29]. COX-2 inhibitor-mediated protection of tumorigenesis is largely due to reduction of synthesis of prostaniod metabolites, especially PGE_2. The most convincing evidence comes from a randomized double-blind placebo-controlled trial, in which celecoxib (COX-2 inhibitor) significantly decreased the incidence of sporadic colorectal adenomas [30].

In the GI tract, administration of PGE_2 or overexpression of COX-2/mPGES-1 increases epithelial cell proliferation and the incidence of Gastric hyperplasia and tumorous growth (aberrant crypt foci, small intestine cancer and colon cancer). Consistently, tumor incidence and growth in the GI tract of genetically modified mice ($cPLA2\alpha$ KO mice, COX-1/2 KO mice and mPGES-1 KO mice) are decreased [31-33]. Mice with COX-2 expression in mammary tissue develop breast cancer. Similarly, DMBA treatment induces less breast tumors in mice that lack COX-2 expression selectively within mammary epithelial cells [34]. In a model of gastric cancer, COX-2 and mPGES-1 are co-expressed in gastric epithelial cells of K19-C2mE transgenic mice [35]. Mucous hyperplastic lesions and gastric adenocarcinomas in the glandular stomach of the mice are significantly increased, especially when the mice are further engineered to express mitogens like Wnt1 or Noggin.

PGE_2 phenotypically acts as an autocrine and/or paracrine mitogen that plays an important role in promoting tumor progression. Several potential mechanisms underlining

the pro-carcinogenic effect of PGE_2 have been reported including: (1) PGE_2 signaling could suppress apoptosis and promote self-sufficient growth of tumor cells. Transactivation of pro-survival signaling downstream of EP receptors might mediate the effect. PGE_2 increases the expression of anti-apoptotic Bcl-2 via activation of the Ras-MAPK/ERK pathway in cancer cells [36-38]. Also, PGE_2 has been reported to activate pro-survival and pro-proliferative pathways including the PI3K/AKT, cAMP/protein kinase A signaling and EGFR signaling [39-41]; (2) PGE_2 contributes to maintenance of tumor stem cells by activation of β-catenin/TCF signaling [42-44]. In colon tumor cells, PGE_2 engages the EP2 receptor to activate PI3K/AKT which sequentially phosphorylates GSK3β and reduces the inhibitory effect of GSK3β-mediated phosphorylation of β-catenin. On the other hand, binding of EP2-associated G-protein αs subunit to Axin promotes β-catenin release from the inhibitory Axin/GSK3β complex. The β-catenin/TCF pathway plays a key role in acquisition of a progenitor or stem cell-like phenotype. PGE_2 signaling helps to establish immortalization and the progression towards the malignant phenotype. (3) PGE_2 induces new blood vessel formation by stimulating production of angiogenic factors such as VEGF and basic fibroblast growth factor [45]. NSAIDs (inhibitors of COX-2) inhibit vascular tube formation from endothelial cells while PGE_2 counteracts the effect [46]. In addition, PGE_2 induces the expression of the pro-angiogenic chemokine CXCL1 in vivo [47]. Therefore, PGE_2 helps maintain tumor mass by promoting angiogenesis. (4) PGE_2 enhances the metastatic phenotype of tumor cells. PGE_2 promotes cytoskeletal reorganization and increases tumor cell migration and invasion via the intracellular Src-mediated transactivation of EGFR/PI3K signaling [48]. Inhibition of COX-2 in vivo attenuates the metastatic potential of colorectal tumors *in*

vivo and *in vitro*. Over-expression of COX-2 in intestinal cells modulates their adhesive properties and increases matrix metalloproteinase activity to promote invasion [49-51]. Moreover, COX-2 has recently been recognized as one of the four "metastasis progression genes" which synergistically promote breast cancer metastasis to the lungs [52]. (5) PGE2 modulation of the innate immune system regulates tumor growth. As previously indicated, PGE_2 inhibits cytokine production by DCs and shifts the Th1 immuno-phenotype to Th2. This immune inhibitory effect may allow tumor cells to escape immune surveillance.

2 PGE_2 in liver disease

One out of every ten Americans is affected by liver disease, among the top ten causes of death in the United States. There are more than 100 liver diseases, including viral hepatitis (HBV, HCV, et.al), fatty liver disease, nonalcoholic steatohepatitis and alcohol-related liver disease. Regardless of the cause, damage to the liver is likely to progress in a similar way. In the early stages, the liver becomes inflamed, tender and enlarged. If left untreated, the inflamed liver will start to scar. As excess scar tissue grows, it replaces healthy liver tissue in a process known as fibrosis. Seriously scarred liver can no longer heal itself. The stage at which the damage cannot be reversed is called cirrhosis. Cirrhosis can lead to a number of complications, including liver failure and liver cancer. inflammation activates innate and adaptive immune responses which stimulate fibrotic differentiation, cellular regeneration, proliferation and mitogen expression. The increased fibrotic immune response and cellular turnover in the context of a noxious environment

leads to an accumulation of scar tissue which replaces normal liver tissue, while also affecting the structure and expression of oncogenes and tumor suppressor genes, leading to liver cancer [53].

Enhanced PGE_2 levels increase the size of the fenestrae in liver sinusoidal endothelial cells, and thereby reinforce liver infiltration by circulating inflammatory cells [54]. Also, PGE_2 downregulates the formation of TNF-α and upregulates the formation of nitric oxide in resident liver macrophages [55]. PGE_2 regulates the differentiation of hepatic stellate cells and has an anti-proliferative effect on hepatic stellate cells, and for this reason might be a useful therapeutic agent against liver fibrosis [56]. Moreover, PGE_2 protects hepatocytes from apoptosis and promotes hepatocyte proliferation, which helps maintain liver integrity [57-60].

An understanding of the mechanisms underlying the regulation of synthesis and release of PGE2 is a prerequisite to interfere in its regulatory functions in liver pathophysiology. COX-1/mPGES-2/cPGES are constitutively expressed in liver tissues,where they maintain a basal of level of PGE_2 production [61]. Inflammatory stimuli induce COX-2/mPGES-1, leading to elevated synthesis of PGE_2, which regulates liver inflammation and tissue homeostasis. Interestingly, normal adult hepatocytes, , fail, both in primary culture and *in vivo,* to express COX-2 upon challenge with pro-inflammatory stimuli, including toll-like receptor ligands and combinations of TNF-α, IL-1β and IFN-γ [5, 62]. This lack of inducibility by pro-inflammatory mediators occurs in adult hepatocytes, but not in hepatocytes from fetal or neonatal animals, or in hepatic-derived stable cell lines. The production of PGE_2 in the liver is accomplished by the expression of COX-2/mPGES-1 in non-hepatocyte cells, with the highest expression

occurring in Kupffer cells and infiltrating macrophages. These observations reinforce the role of liver infiltration by circulating inflammatory cells in the release of PGE_2.

2.1 PGE_2 in liver inflammation and regeneration

As previously stated, PGE_2 supports acute liver inflammation and phagocyte-mediated immunity at the site of pathogen entry, but it has a specialized role in controlling the potentially harmful activation of CTL-, Th1-, and NK cell-mediated type-1 immune response, especially at later stages [2]. Such PGE_2-mediated suppression of type-1 immunity by PGE_2 shifts the pattern of immune reactivity toward a less aggressive form of immunity mediated by Th2 and Th17 cells, as well as enhancement of the Treg- and myeloid-derived suppressor cells-mediated suppressive events [63]. Although PGE_2 can accelerate DC maturation and migratory function, the PGE_2-dependent suppression of the T cell-attracting chemokine, CCL19, in DCs and its suppression of IL-2 and IL-12 production result in the net inhibitory activity of PGE_2 during the induction of adapted immunity [2]. In accordance with PGE_2 phase specific regulatory function, liver specific COX-2 transgenic mice exhibit a more severe acute liver injury after LPS/GalN administration [64], while they are protected against E coli infection induced chronic liver inflammation [65]. In the former case, enhanced PGE_2 promotes acute onset of inflammation, which is exacerbated by the hepatotoxicity of GalN. In the latter case, PGE_2 inhibits the emergence of T cells in the peritoneal cavity, which are important for host defense against E. coli, and prevents bacterial exclusion in the peritoneal cavity after E. coli challenge. More direct evidence of the PGE_2 immunosuppressive role in liver

disease comes from recent studies of PGE_2 dependent immunological tolerance in mice with concanavalin A-induced immune-mediated liver injury. The immunological tolerogenic effect of $dmPGE_2$ is proved in C57B/6 male mice with Con A-induced liver injury, and was partially associated with the expression of IL-10, an anti-inflammatory cytokine, in Kupffer cells [66].

There are cumulative studies supporting the proliferative and anti-apoptotic role of PGE_2 in different models of liver failure as well as after ischemia/reperfusion injury. Recently, the COX-2 gene has been expressed under the control of different specific promoters: apolipoprotein E, transthyretin or the albumin-enhancer promoter, all 3 models giving a high liver-specificity in the expression of the transgene [64, 67, 68]. A very potent protection against liver injury and animal death was observed in those animals that carried the COX-2 transgene, through a mechanism that involved Src/epidermal growth factor receptor signaling. Moreover, partial hepatectomy promoted a rapid expression of COX-2 and synthesis of PGE_2 in hepatocytes that contribute to onset of regeneration [69]. This is confirmed by the impaired recovery observed after administration of selective COX-2 inhibitors or in animals lacking the COX-2 gene [70]. COX-2-deficient animals exhibited a full recovery of liver mass and function after partial hepatectomy with a delayed early commitment to proliferation. The simultaneous absence of COX-2 and other genes relevant for liver regeneration, such as nitric oxide synthase-2 resulted in an impaired liver mass recovery after partial hepatectomy, leading to animal death. Similarly, Zhang et al. reported that elevating PGE_2, either by deleting or inhibiting 15-PGDH, increases liver regeneration in mouse models [25].

2.2 PGE$_2$ in liver cancer

HCC and intrahepatic cholangiocarcinoma are the two major forms of primary liver cancers, accounting for approximately 90% and 5% respectively [71]. The tumorigenic process of HCC is characterized by dysregulation of hepatocyte cell cycle progression and abnormal hepatocyte proliferation in the setting of chronic inflammation and fibrosis of the liver parenchyma [72]. Cholangiocarcinoma is a highly malignant cancer of the biliary tract. The tumor often arises from background conditions that cause long-standing inflammation, injury and reparative biliary epithelial cell proliferation, such as primary sclerosing cholangitis, clonorchiasis, hepatolithiasis or complicated fibropolycystic disease [73]. Several lines of evidence suggest PGE$_2$ is implicated in both types of hepatic carcinogenesis.

2.2.1 PGE$_2$ in HCC

Increased COX-2 expression has been found in human and animal HCCs. Elevated levels of PGs, most notably PGE$_2$, have also been detected in liver cancer cells [74-77]. Furthermore,COX-2 promotes the growth of human HCC cells. Transfection of human HCC cell lines (Hep3B and HepG2) with a COX-2 expression vector or treatment with exogenous PGE$_2$ induces phosphorylation of Akt and enhances cell growth. Secondly, overexpression of COX-2 or treatment with exogenous PGE$_2$ increases human HCC invasiveness [78]. The observations that PGE$_2$-induced HCC migration was blocked by inhibitors of MEK/ERK, p38 MAPK, protein kinases A and C, suggests the involvement of multiple protein kinases in the process [79]. In addition, two recent

studies show that elevated COX-2 expression correlates with increased VEGF levels and microvascular density in human HCCs. In cultured hepatocellular carcinoma cells, overexpression of COX-2 or treatment with PGE_2 enhances VEGF production and this effect is blocked by inhibition of COX-2 [80]. Consistent with previous results, selective COX-2 inhibitors (such as celecoxib) inhibit proliferation and induce apoptosis in cultured hepatocellular carcinoma cells. It is suggested that celecoxib treatment decreased PGE_2 mediated phosphorylation of Akt and that inhibition of Akt reduced HCC cell viability [76]. Also, the COX-2 inhibitors exert a chemopreventive effect in hepatocarcinogenesis models [81-83].

Elevated expression of mPGES-1 has also been found in several human cancers including HCC [84]. Consistent with the documented role of mPGES-1 in PGE_2 synthesis, mPGES-1 knockdown has been shown to inhibit PGE_2 production and reduce HCC cell proliferation and/or invasiveness [85, 86]. mPGES-1 overexpression is suggested to enhance HCC cell proliferation through PGE2-mediated activation of EGR1 and the β-catenin signaling pathway. Overexpression of mPGES-1 or treatment with PGE_2 induces the formation of an EGR1/β-catenin complex, which interacts with TCF4/LEF1 transcription factors and activates the expression of β-catenin downstream genes [85].

Furthermore, overexpression of 15-PGDH inhibited HCC cell growth *in vitro*, whereas knockdown of 15-PGDH enhanced tumor growth [11]. In a tumor xenograft modelin SCID mice, inoculation of human HCC cells (Huh7), overexpressing 15-PGDH led to significant inhibition of tumor growth, while knockdown of 15-PGDH enhanced tumor growth. In a separate tumor xenograft model in which mouse HCC cells (Hepa1-6) were inoculated into syngeneic C57BL/6 mice, intratumoral injection of adenovirus

vector expressing 15-PGDH (pAd-15-PGDH) significantly inhibited xenograft tumor growth. The anti-tumor effect of 15-PGDH is mainly dependent on degradation of pro-carcinogenic PGE_2. Furthermore, 15-PGDH-derived 15-keto-PGE_2 enhanced the association of PPARγ with the p21WAF1/Cip1 promoter and increased p21 expression and association with CDK2, CDK4 and PCNA. Depletion of p21 by shRNA reversed 15-PGDH-induced inhibition of HCC cell growth, while overexpression of p21 prevented 15-PGDH knockdown-induced tumor cell growth.

2.2.2 PGE_2 in cholangiocarcinoma

Immunohistochemical studies demonstrate enhanced COX-2 expression in cholangiocarcinoma cells and pre-cancerous bile duct lesions but not in normal BECs [73]. Positive immunostaining for COX-2 is observed in the cytoplasm of human cholangiocarcinoma cells and bile duct epithelium of PSC patients, whereas normal intrahepatic biliary epithelium of matched non-tumorous controls or normal liver specimens showed only weak COX-2 expression [87-89]. Elevated COX-2 expression is also observed in furan-induced cholangiocarcinoma in rats. Activation of EGFR has been proposed as an important mechanism for upregulation of COX-2 and PGE_2 production in human cholangiocarcinoma cells [90, 91]. Overexpression of COX-2 in cultured human cholangiocarcinoma cells enhances PGE_2 production and promotes tumor growth, whereas antisense depletion of COX-2 reduces cholangiocarcinoma cell proliferation. COX-2/PGE_2 inhibits Fas-ligand-mediated apoptosis in cultured cholangiocarcinoma cells through upregulating Mcl-1, an anti-apoptotic member of the Bcl-2 family.

Treatment of cholangiocarcinoma cells with exogenous PGE_2 increases tumor cell growth and prevents apoptosis [92-94]. Prostaglandin signaling also mediates HGF and IL-6-induced cholangiocarcinoma cell growth [95].

On the other hand, mPGES-1 is also overexpressed in human cholangiocarcinoma tissues [96]. Overexpression of mPGES-1 in human cholangiocarcinoma cells increased tumor cell proliferation, migration, invasion, and colony formation; in contrast, RNAi knockdown of mPGES-1 inhibited tumor growth. In SCID mice with tumor xenografts, mPGES-1 overexpression accelerated tumor formation and increased tumor weight, whereas mPGES-1 knockdown delayed tumor formation and reduced tumor weight. mPGES-1 inhibited the expression of PTEN, leading to activation of the EGFR/PI3K/AKT/mTOR signaling pathways in cholangiocarcinoma cells. mPGES1 mediated inhibition of PTEN is regulated through blocking EGR-1 sumoylation and subsequent binding to the 5'-UTR of the PTEN gene.

Lastly, overexpression of 15-PGDH in cholangiocarcinoma cells inhibits tumor cell growth *in vitro* and *in vivo* [12]. A novel 15-PGDH/15-keto-PGE_2-mediated signaling cascade that interacts with peroxisome proliferator-activated receptor-γ (PPAR-γ), Smad2/3, and TAP63 in human cholangiocarcinoma cells has recently been pusblised. The role of TAP63 in 15-PGDH/15-keto-PGE_2-induced inhibition of tumor growth was further supported by the observation that knockdown of TAP63 prevented 15-PGDH-induced inhibition of tumor cell proliferation, colony formation, and migration. Given that 15-PGDH converts the pro-inflammatory and pro-tumorigenic PGE_2 to the anti-inflammatory and tumor-suppressive 15-keto-PGE_2, induction of endogenous 15-PGDH

expression or delivery of exogenous 15-PGDH/15-keto-PGE$_2$ may be therapeutic for treatment of liver cancer.

CHAPTER 2 MATERIALS AND METHODS

1. Materials

Dulbecco's modified minimum essential medium (DMEM) and fetal bovine serum (FBS) were purchased from Sigma (St. Louis, MO). Williams' Medium E medium, Opti-MEM reduced serum medium, RPMI-1640 medium, puromycin and Lipofectamine™ 2000 reagent were purchased from Invitrogen (Carlsbad, CA). Docosahexaenoic acid (DHA) and arachidonic acid (AA) were purchased from Cayman Chemical (Ann Arbor, MI). miR26a and miR26b lentiviral particles were purchased from GeneCopoeia (Rockville, MD). 15-PGDH 3'UTR-luciferase reporter was obtained from ORIGENE (Rockville, MD). Rabbit polyclonal antibody against 15-PGDH was purchased from Cayman chemical (Ann Arbor, MI). Rabbit polyclonal antibody against c-myc was purchased from Santa Cruz Biotechnology (Dallas, TX). Mouse monoclonal antibodies against CTDSPL and CTDSP1 were purchased from Abcam (Cambridge, MA). Mouse monoclonal antibodies against β-actin were purchased from Sigma-Aldrich (St. Louis, MO). Rabbit monoclonal antibody against 15-PGDH/mPGES-1 used in immunohistochemical procedure was purchased form Novus Biologicals (Littleton, CO). anti-Fas antibody Jo2 was purchased from BD Bioscience (Franklin Lakes, NJ). siRNA against 15-PGDH was synthesized by ORIGENE (Rockville, MD). lipopolysaccharides (LPS) and D-galactosamine (D-GalN) were purchased from Sigma-Aldrich (St. Louis,

MO). 15-PGDH inhibitor and Akt inhibitor V were purchased from EMD Millipore (Billerica, MA). mPGES-1 inhibitor MF63 were purchased from Abmole bioscience (Houston, TX). C57BL/6 wild type mice and NOD CB17-prkdc/SCID mice were purchased from Jackson lab (Bar Harbor, Maine) and maintained in Tulane transgenic mice facility according to the protocol approved by the American Association for Accreditation of Laboratory Animal Care. All primers used in this study were synthesized by Integrated DNA Technologies (IDT, Coralville, IA). All chemical reagents were analytical grade (Sigma, St. Louis, MO).

2. **Cell culture**

Two human cholangiocarcinoma cell lines, CCLP1 and TFK-1, were used in this study. CCLP1 was maintained in DMEM (life technology, Grand Island, NY) supplemented with 10% heat-inactivated fetal bovine serum (Sigma, St. Louis, MO). TFK-1 was maintained in RPMI-1640 (life technology, Grand Island, NY) containing 10% heat-inactivated fetal bovine serum. CCLP1 and TFK-1 cells were transfected with Fat-1 expression plasmid or control vector pcDNA3 and then maintained in complete culture medium with 0.2 ug/ml puromycin (life technology, Grand Island, NY). CCLP1 and TFK-1 cells were also infected with miR26a/b lentivirus or miRNA-scramble control and the cells were maintained in culture medium with 0.2 mg/ml Geneticin (life technology, Grand Island, NY). Medium is replaced every 3 days for 2-4 weeks until outgrowth of resistant cells. The resistant cells were harvested and maintained in culture media with selection agents for further use.

3. Animal studies

Transgenic mice with expression of mPGES-1/15-PGDH gene in hepatocytes were developed by pronuclear injection of the mPGES-1/15-PGDH transgene construct into fertilized mouse eggs of B6D2F1 background at the single cell stage. Specifically, human mPGES-1/15-PGDH cDNA was ligated to the mouse albumin promoter/enhancer and the construct was microinjected into the pronuclei during the window of time the eggs were visible within the protoplasm. The injected eggs were then transferred into the oviducts of pseudopregnant foster mice. The pups born to the foster mothers with genomic integration of the injected DNA were identified by using tail DNA samples and become transgenic founder mice. The founder was backcrossed with the C57BL/6 wild type mice for more than five consecutive generations to produce incipient congenic mPGES-1/15-PGDH Tg mice (B6, ALB-hu- mPGES-1/15-PGDH). All experimental animals used in this study were handled according to the protocol approved by Institutional Animal Care and Use Committee of Tulane University.

To develop Fas-induced liver injury, male mice at the age of 8–10 weeks were injected intraperitoneally with 0.5 µg/g of body weight the anti-Fas antibody Jo2 (BD Bioscience, Franklin Lakes, NJ) (Jo2 was dissolved in sterile 1×Dulbecco's Phosphate Buffered Saline). After Jo2 injection, the mice were followed for 12h for survival analysis or sacrificed at 5h to obtain blood and liver tissue samples. For inhibitor treatment, mice were injected intraperitoneally with Akt inhibitor V (1µg/g body weight) (Merck Millipore, Billerica, MA) at 2 h before Jo2 injection, or were administrated via

oral gavage with mPGES-1 inhibitor MF63 (50µg/g body weight, twice every 12 h) (Abmole bioscience, Houston, TX) before Jo2 injection.

To develop endotoxin induced liver injury model, mice were administered intraperitoneally with 60ng/g body weight lipopolysaccharides (LPS) (Sigma-Aldrich, St. Louis, MO) in combination with 800µg/g body weight of D-galactosamine (D-GalN) (Sigma-Aldrich, St. Louis, MO) (LPS and D-GalN were dissolved in sterile, nonpyrogenic 0.9% sodium chloride solution). After LPS/GalN injection, the mice were followed for 24h for survival analysis or sacrificed at 5h to obtain blood and liver tissue samples.

4. Gene expression analysis

Total RNA was extracted from either liver tissue samples or cultured cells according to TRIzol® Reagent method (life technology, Grand Island, NY). mRNA levels were quantified by using RT² SYBR® Green qPCR kit (QIAGEN, Germantown, MD); GAPDH is used as internal control. miRNA levels were quantified by using miScript Primer Assays kit (QIAGEN, Germantown, MD); U6 was measured as reference gene.

For Western blotting analyses, liver tissue samples or cultured cells were homogenized and lysed by NP-40 lysis buffer or RIPA lysis buffer. All lysis buffers were prepared with the protease inhibitor cocktail and phosphatase inhibitor cocktail (Roche Diagnostics, Indianapolis, Indiana). Cellular proteins were separated by SDS-PAGE electrophoresis and transferred onto nitrocellulose membranes (Bio-Rad, Hercules, CA).

The membranes were blocked by PBS-T (0.5% Tween 20 in PBS) containing 5% nonfat milk for 1h at room temperature, and then incubated with individual primary antibodies in PBS-T containing 5% nonfat milk for 2-5h at room temperature with the dilutions specified by the manufacturers. Following three washes with PBS-T, the membranes were incubated with IRDye 680LT/IRDye 800CW secondary antibodies (LI-COR Biosciences, Lincoln, NE) in PBS-T for 1 h at room temperature. The membranes were then washed with PBS-T and the protein bands were visualized by using the ODYSSEY infrared imaging system (LI-COR Biosciences, Lincoln, NE).

5. Dual-Luciferase Reporter Assay

Cells were co-transfected with luciferase reporter (15-PGDH promoter-luciferase, 15-PGDH 3'UTR-luciferase) and pRL-TK (Promega, Madison, WI). pRL-TK provides the constitutive expression of Renilla luciferase that was used as an internal control. 72h after transfection, cells were collected and passively lysed. Luciferase activities in the extracts were measured by DLReady Centro XS3 LB960 luminometer with the use of Dual-Luciferase Reporter (DLR™) Assay kit (Promega, Madison, WI). Luciferase activity was measured against Renilla luciferase activity for transfection efficiency.

6. ChIP Assay

Cells were cross-linked by 1% formaldehyde for 10min. Chromosome DNA was extracted according to the protocol provided by SimpleChIP Assay Kits (Cell signaling,

Danvers, MA) and precipitated by using specific c-myc Rabbit polyclone antibody. Rabbit polyclone antibody Histone 3 was used as positive control while Rabbit IgG was used as negative control. Regular PCR procedure (5min at 94°C, followed by 30 cycles of 30s at 94°C, 30s at 55°C, 30s at 72°C, ended by 10min at 72°C) was adopted to amplify the c-myc binding site sequence.

7. Cell proliferation assay

5×10^3 cells were plated in each well of 96-well plates and synchronized in G0 phase by serum deprivation. Growth arrest was released by adding 2% serum. WST-1 reagent (Roche Diagnostics, Indianapolis, Indiana) was used to detect cell proliferation rate according to the manufacturer's instructions. Each point in cell growth curve represents the mean of three independent normalized OD450 reads.

8. Colony forming Assay

1×10^3 cells were plated in 10-cm dish and allowed to grow for 14 days. The colonies were stained with crystal violet (Amersco, Solon, OH). The colonies in each dish were counted.

9. Cell invasion assay

1×10^3 cells were seeded in Matrigel Invasion Chambers (BD, Franklin Lakes, NJ) which were placed in 24-well plates containing 0.5 ml DMEM medium with 2%

serum. After 24 hours the invaded cells were fixed and stained (H&E). The numbers of invaded cells were counted from five randomly selected fields under microscope (×400).

10. TUNEL assay

Cultured human cholangiocarcinoma cells (1×104 per well) were seeded in 8 wells chamber slide and cultured overnight. Then, Cells were fixed by 4% formaldehyde in PBS for 25min and cell Apoptosis on the slide was detected according to the protocol of DeadendTM colorimetric TUNEL system (Promega, Madison, WI).

Isolated primary hepatocyte was fixed in 4% formaldehyde for 25 minutes at 4°C. TUNEL staining of fixed cell was performed using DeadEnd™ Fluorometric TUNEL System (Promega, Madison, WI). The apoptotic index was calculated as the percentage of positively stained cells.

11. Xenograft tumor study in SCID mice

SCID mice were injected subcutaneously at the axillary area with indicated groups of CCLP1 cells (1×107 cells in 100μl of PBS). The mice were closely monitored for tumor growth and sacrificed 35 days post inoculation to recover the tumors. The tumor volume was measured and calculated by using the formula: larger diameter × (smaller diameter)2/2. RNA was extracted from recovered tumor tissues using TRIzol® Reagent (life technology, Grand Island, NY) to measure the level of miR-26a. Proteins

from the tumor tissues were extracted by using NP-40 lysis buffer for Western blotting analysis.

12. Intrahepatic tumor growth via splenic injection

General anesthesia in mice was induced by Fluriso (Vetone, BOISE, ID). The abdominal cavity was opened by a 0.5 cm left sided transverse laparotomy. The spleen was identified, and 1×106 cells (with or without 15-PGDH knockdown) in a total volume of 100μl PBS were injected into the spleen. After tumor cell inoculation, the spleen was resected and the abdominal cavity was closed by a running 3/0 braided silk suture (CP medical, Portland, OR). The mice were intraperitoneally injected with 200μl DHA (0.5mg/ml, dissolved in BSA solution) or BSA control every 2 days (starting 2 days after surgery). Five weeks after DHA treatment, the mice were sacrificed and the livers were removed to document tumor growth parameters (tumor volume was calculated by using the formula: larger diameter $\times$ [smaller diameter]^2/2).

13. ALT/AST analysis

Blood samples were centrifuged at 3000 rpm for 15 minutes to obtain serum. Serum alanine aminotransferase (ALT) and aspartate aminotransferase (AST) levels were measured with an automatic analyzer at the Department of Clinical Chemistry, Tulane University Hospital.

14. Immunohistochemical procedure

Liver tissues were fixed in 10% buffered formalin and embedded in paraffin. Sections (4μm) were deparaffinized and processed for hematoxylin-eosin (H&E) staining and immunohistochemistry. Antibodies were diluted in 1×PBS containing 4% horse serum, 0.2% Triton-X100 and 0.4mg/ml methiolate. mPGES-1 antibody (1:200, Novus Biologicals, Littleton, CO) was used to detect mPGES-1 expression. 15-PGDH antibody (1:500, Novus Biologicals, Littleton, CO) was used to detect 15-PGDH expression. Cleaved caspase-3 antibody (1:200, Biocare Medical, Pike Lane Concord, CA) was used to detect apoptosis. . F4/80 antibody (1:200, abcam, Cambridge, MA) was used to detect macrophage. Horseradish peroxidase–conjugated goat anti-rabbit IgG was used as secondary antibody. Signals were visualized using 0.2mg/mL diaminobenzidine, 0.01% hydrogen peroxide in 0.1 M phosphate buffer.

15. Caspases Activities Analysis

Liver protein extracts were prepared as previous described [97]. Caspase-3/7, caspase-8 and caspase-9 activities were measured with Caspase-Glo Assay kit (Promega Corporation, Madison, WI). The caspase activities were expressed as fold changes over the control (corresponding wild type mice).

16. Isolation and culture of primary mouse liver cells

Hepatocytes were isolated by an adaptation of the calcium two-step collagenase perfusion technique as described previously [27]. Collagen I coated plates and dishes

were purchased form BD Biosciences (San Jose, CA). 1×106, 3×106, or 2.5×104 hepatocytes were plated onto collagen-coated 6-well plates, 10-cm dishes, or 96-well plates, respectively. Hepatocytes were maintained in Williams' Medium E medium (Invitrogen) supplemented with Hepatocyte Maintenance Supplement Pack (Invitrogen), 10% fetal calf serum (Sigma), 2mM L-Glutamine (Invitrogen) and Antibiotics (Invitrogen).

For Kupffer cell isolation, collagenase-perfused liver tissues were further digested in RPMI-1640 (life technology, Grand Island, NY) containing 0.1% type IV collagenase for 30min at 37◦C. The liver homogenate was filtered and centrifuged at $50\times g$ for 5min. The top aqueous phase was reserved and centrifuged at $1400\times g$ for 10min; the cell sediment mainly contained Kupffer cells. The cells were suspended and maintained in 6-well plate at a density $1\text{-}3\times106$ /well in DMEM (life technology, Grand Island, NY) supplemented with 10% heat-inactivated fetal bovine serum (Sigma, St. Louis, MO).

17. Prostaglandin E Metabolite assay

Isolated hepatocytes were cultured in serum-free medium with/without supplementation of Arachidonic acid (AA) (10μM) and/or 15-PGDH inhibitor (EMD Millipore, Billerica, MA) (1μM) for 12h. Before collecting culture medium, cells were stimulated with Calcium ionophore A23187 (100μM) for 10min. Prostaglandin E Metabolite concentration in culture medium was analyzed according to instruction of Prostaglandin E Metabolite EIA Kit (Cayman, Ann Arbor, Michigan).

18. Prostaglandin E assay

Isolated hepatocytes were cultured in serum-free medium with or without supplementation of arachidonic acid (AA) (10μM) and/or the mPGES-1 inhibitor MF63 (1μM) (Cayman, Ann Arbor, Michigan) (1μM) for 12h. Before collecting culture medium, cells were stimulated with calcium ionophore A23187 (100μM) for 10min. Prostaglandin E concentration in culture medium was analyzed according to instruction of the Prostaglandin E_2 ELISA kit (Abcam, Cambridge, MA).

19. ROS Assay

Hepatocytes were seeded at 2.5×104 cells/well on 96 well plates. ROS Assay of adherent cells was performed using DCFDA Cellular ROS Detection Assay Kit (Abcam, Cambridge, MA). Signal was collected at 485 nm/535 nm by FLUOstar omega (BMG labtech, Cary, NC). The data are expressed as percentage of fold change.

20. EMSA

Nuclear protein is prepared by nuclear extraction kit (EMD millipore, Darmstadt, Germany). EMSA was processed according to the protocol of The Gelshift Chemiluminescent EMSA Assay Kit (Active Motif, Carlsbad, CA).

21. Statistical Analysis

Data are presented as mean ± standard error. Differences between two groups were determined by a two-tailed Student's t test. Kaplan-Meier survival analysis was used for mortality analysis. A value of $p < 0.05$ was considered to be statistically significant.

CHAPTER 3 RESULTS

PART I. Microsomal prostaglandin E synthase-1 (mPGES-1) protects against Fas-induced liver injury

1. Development of mPGES-1 transgenic mice

We developed transgenic mice (Tg) with targeted expression of mPGES-1 in the liver by pronuclear injection of a mPGES-1 transgene construct (under the control of albumin promoter/enhancer) into fertilized mouse eggs at the single cell stage (Figure 1A). Successful expression of mPGES-1 in the liver tissues from the transgenic mice was confirmed by immunohistochemical staining. Consistent with the enzymatic action of mPGES-1 for PGE_2 synthesis, hepatocytes isolated from the mPGES-1 Tg mice showed higher levels of PGE_2 production compared to WT hepatocytes; this effect was augmented when the hepatocytes were incubated with arachidonic acid (AA), the substrate for PG synthesis. Conversely, the production of PGE2 in the mPGES-1 Tg hepatocytes was decreased by treatment with the mPGES-1 inhibitor, MF63 (Figure 1B-D). These findings demonstrate that the mPGES-1 Tg mice express functional mPGES-1 in hepatocytes.

Figure 1

A

Superovulated and fertilized female (B6D2F1)

fertilized eggs at the single cell stage

Birth of transgenics

Founder selection (B6D2;ALB-hu-mPGES-1)

Establishing incipient congentic strains

B6D2;ALB-hu-mPGES-1   C57B6/6J

5 times

Incipient congentic strains (B6, ALB-hu-mPGES-1)

B

750bp
500bp
250bp

C

Wild type   mPGES-1 Tg

Negative control

mPGES-1

D
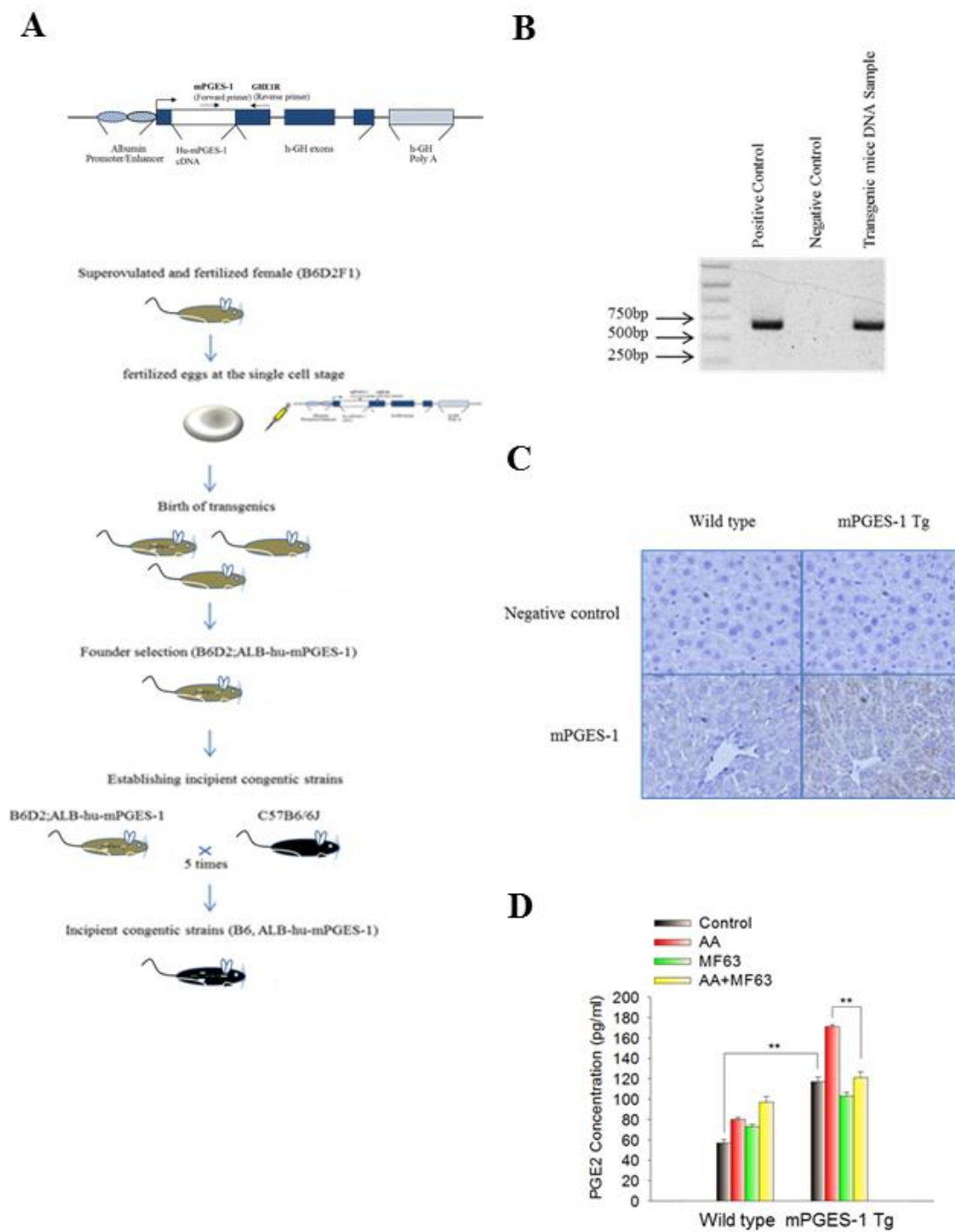
Figure 1. Development of liver specific mPGES-1 Tg mice.

(A) Schematic presentation of the strategy to develop mPGES-1 transgenic mice as described in the Methods. (B) Representative gel image of PCR genotyping. 0.5 cm pup tail were cut and digested for isolation of genome DNA. PCR was performed to amplify partial sequence of inserted mPGES-1 gene with specific primers. (C) Representative images of immunohistochemical stain for mPGES-1 in liver tissue sections. (D) PGE_2 concentration in the media from cultured hepatocytes isolated from wild type and mPGES-1 Tg mice. The hepatocytes were incubated with or without the arachidonic acid substrate (10µM) and treated with or without the mPGES-1 inhibitor MF63 (1µM). The data are expressed as mean±SE, **$p<0.01$.

2. Hepatic overexpression of mPGES-1 protects mice against Fas-induced liver injury

To investigate the effect of mPGES-1 in Fas-induced liver injury, mPGES-1 Tg mice and their age/sex matched wild type mice were intraperitoneally injected with a single-dose of Fas monoclonal antibody Jo2 and the animals were closely monitored for mortality. We observed that the mPGES-1 Tg mice had a higher survival rate (60%) compared to the WT mice (0% survival rate; all WT mice died by 8h) (P value=1.38e-3, Kaplan-Meier survival analysis) (Figure 2A).

On the basis of the survival curve, additional groups of animals were sacrificed at 5h after Jo2 injection to collect blood and liver tissues for evaluation of liver injury. Upon Jo2 treatment, mPGES-1 Tg mice exhibited less liver injury, as evidenced by less hemorrhagic appearance under gross examination (Figure 2B), lower serum alanine transaminase (ALT) and aspartate transaminase (AST) levels (Figure 2C), less liver tissue injury under histological examination (H&E staining) (Figure 2D), and lower level of apoptosis as determined by PARP cleavage (Figure 2E), immunohistochemical staining for cleaved caspase-3 (Figure 2F), and caspase activity assays (Figure 2G). These results demonstrate that hepatic overexpression of mPGES-1 protects mice against Fas-induced hepatocyte apoptosis and liver injury.

We next utilized a complementary pharmacological approach to further determine the role of mPGES-1 in Fas-induced liver injury. Specifically, the mice were pre-treated with MF63, a pharmacological inhibitor of mPGES-1, prior to Jo2 injection. For this protocol, two doses of MF63 were administrated via oral gavage (every 12h) before Jo2

injection and the mice were sacrificed 5 hours after Jo2 injection (outlined in Figure 3A). We observed that MF63 pretreatment partially reversed the resistance of mPGES-1 Tg mice to Jo2-induced liver injury (Figure 3B-G). These findings further support the role of mPGES-1 in modulation of Fas-induced hepatocyte apoptosis and liver injury.

Figure 2
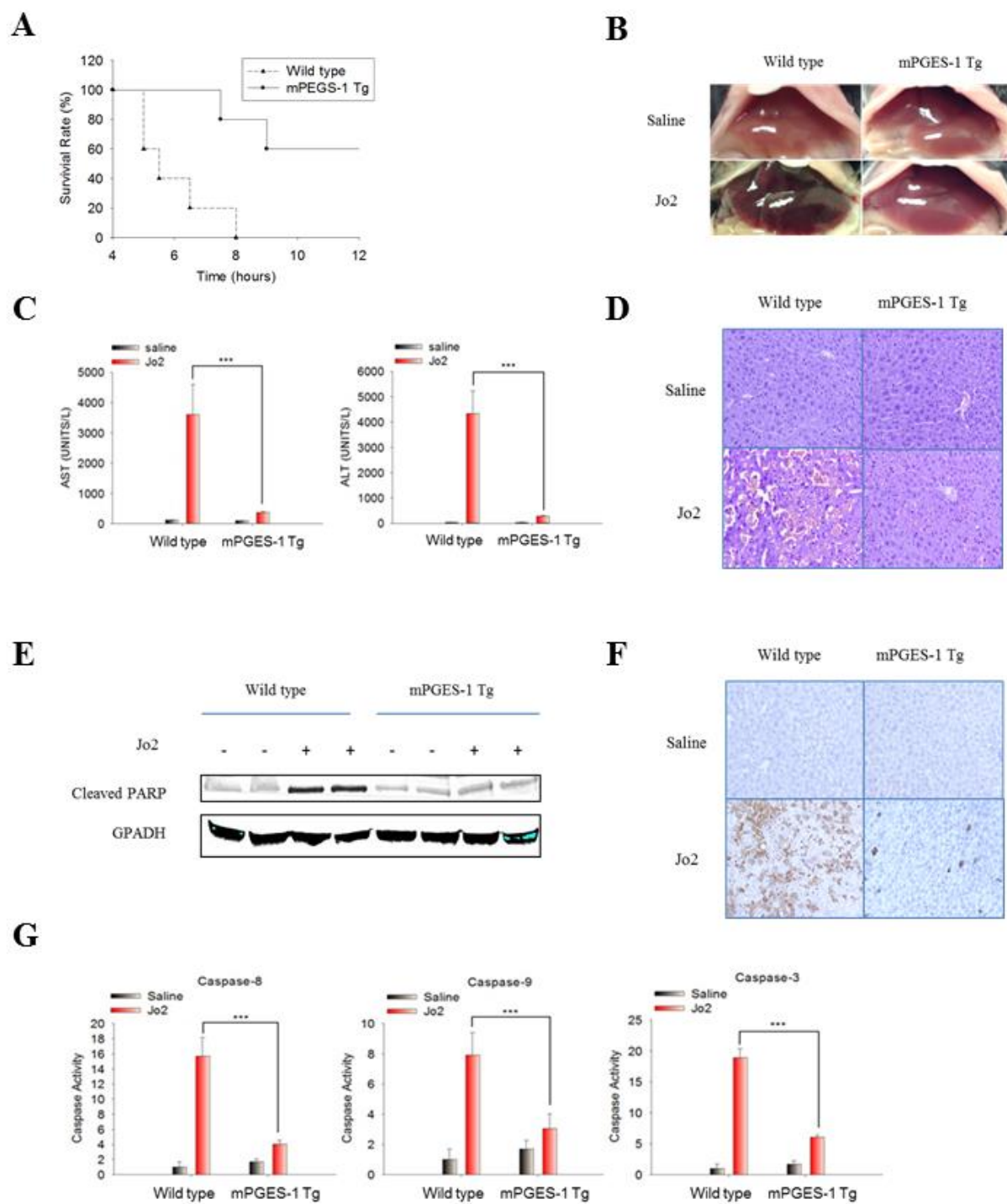
Figure 2. Hepatic overexpression of mPGES-1 protects mice against Fas-induced liver injury.

mPGES-1 Tg mice and their age/sex matched WT mice were intraperitoneally injected with a single dose of purified hamster anti-mouse Fas monoclonal antibody Jo2 (0.5 µg/g body weight). Following Jo2 injection, the mice were closely monitored for survival. Separate groups of mice were sacrificed at 5h after Jo2 injection to collect serum and liver tissue samples.

(A) Survival curve of mice after Jo2 injection. (B) Representative gross images of livers from different groups of mice. (C) Serum ALT and AST levels. The data are expressed as mean±SE from three mice per group (*** $P<0.001$). (D) Representative microscopic images of liver tissue sections (H&E stain). (E) Protein level of cleaved PARP in liver tissue homogenates as determined by Western blotting analysis. GAPDH was used as loading control. (F) Representative images of immunohistochemical stain for cleaved caspase-3 in liver tissues. (G) Caspase-9, 8, and 3 activities in liver tissue homogenates. The results are presented as mean ± SE of fold changes over saline-treated wild type group, *** $P<0.001$.

Figure 3

A

B

C

D

E

F

G
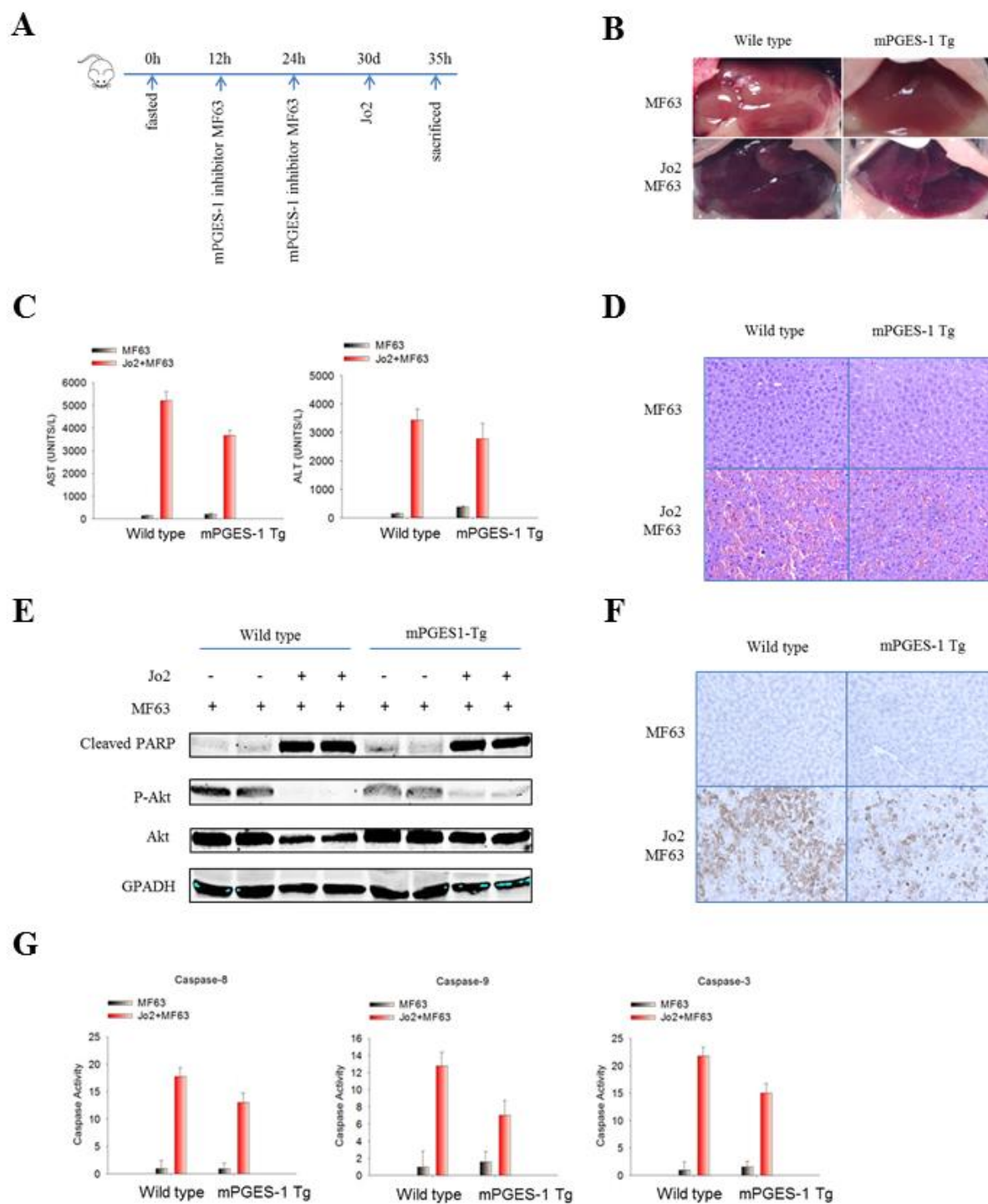
Figure 3. The mPGES1 inhibitor, MF63, restores the susceptibility of mPGES-1 Tg mice to Fas-induced liver injury.

mPGES-1 Tg mice and their age/sex matched WT controls were fasted overnight. The mPGES1 inhibitor MF63 (50μg/g body weight) was administrated via oral gavage (twice every 12 h) before Jo2 (0.5 ug/g body weight) injection. Mice were sacrificed at 5 h after Jo2 injection to collect serum and liver tissue samples.

(A) Timeline of the experiments. (B) Representative gross images of livers from different groups of mice. (C) Serum ALT and AST levels. The data are expressed as mean±SE from three mice per group. (D) Representative microscopic images of liver tissue sections (H&E stain). (E) Protein levels of cleaved PARP, P-Akt and Akt in liver tissue homogenates by Western blotting analysis. GAPDH was used as loading control. (F) Representative images of immunohistochemical stain for cleaved caspase-3 in liver tissues. (G) Caspase-9, 8, and 3 activities in liver tissue homogenates. The results are expressed as mean ± SE of fold changes over MF63-treated wild type group.

3. Hepatic overexpression of mPGES-1 enhances EGFR/Akt signaling

PGE2 is known to activate EGFR/Akt cascade and enhance hepatic cell survival[17, 37]. Accordingly, activation of EGFR/Akt is able to induce the expression of several anti-apoptotic molecules, including Bcl-xl and Mcl-1[38-40]. In our system, we postulate that mPGES-1 may render hepatocytes resistant to apoptosis via activation of the EGFR/Akt pathway. To evaluate for this possibility, we performed Western blotting analysis to determine the levels of EGFR/Akt and associated apoptosis-regulatory molecules. Under baseline condition (i.e., without Jo2 treatment), the mPGES-1 Tg and WT livers showed similar levels of EGFR expression/phosphorylation (Figure 4). Following Jo2 treatment, while the levels of EGFR and p-EGFR in the WT livers became decreased, the mPGES-1 Tg livers showed sustained EGFR expression and phosphorylation. Consistent with the activation of Akt by EGFR, the levels of hepatic p-Akt and associated anti-apoptotic molecules (Mcl-1, Bcl-xl, p-Bad) in Jo2-treated mPGES-1 Tg mice were higher compared to Jo2-treated WT mice (Figure 4). These findings indicate an important role of Akt and associated apoptosis-regulatory molecules in mPGES-1-mediated protection against liver injury. In support of this view, inhibition of mPGES-1 by MF63 reduced Akt expression/phosphorylation in the liver tissues (Figure 3F) and hepatocytes (Figure 6) of mPGES-1 Tg mice. Taken together, our findings demonstrate that mPGES-1 signaling upregulates and activates Akt in hepatocytes which are important for prevention of Fas-induced liver injury.

Figure 4
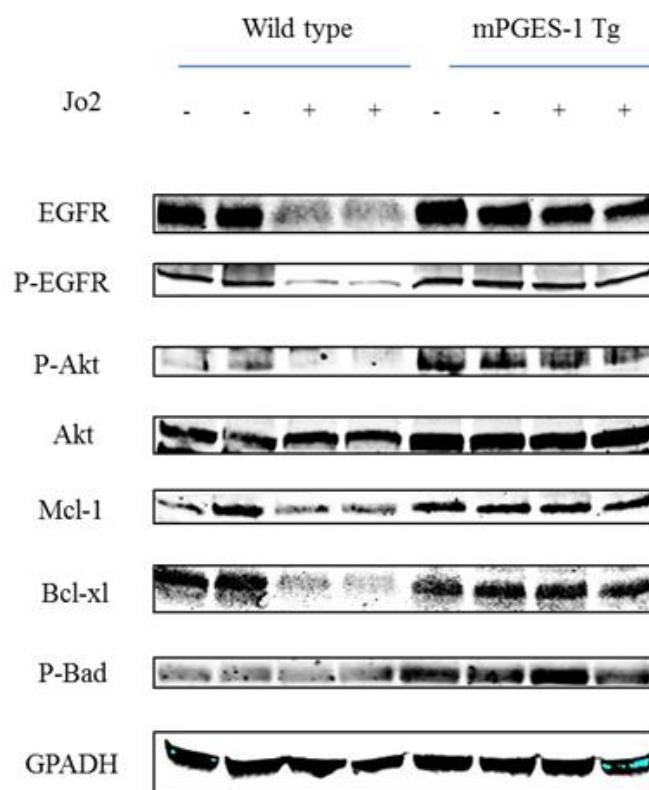
Figure 4. The levels of EGFR, Akt and related molecules.

Equal amounts of the liver tissue proteins were subjected to SDS-PAGE and Western blotting analysis to determine the levels of EGFR, p-EGFR, Akt, p-Akt, Mcl-1, Bcl-xl and p-Bad. GAPDH was measured as the loading control.

4. Inhibition of Akt reverses mPGES-1-mediatated resistance to Fas-induced liver injury.

To further determine the role of Akt in mPGES-1-mediated resistance to Fas-induced liver injury, we employed a pharmacological inhibitor of Akt in our system. Specifically, Akt inhibitor V was intraperitoneally injected to WT and mPGES-1 Tg mice 2 hours prior to Jo2 injection (outlined in Figure 5A); 5 hours after Jo2 injection the blood and liver tissues were collected to determine the extent of liver injury. We observed that pretreatment with Akt inhibitor V reversed the resistance of mPGES-1 Tg mice to Fas-induced liver injury (Figure 5B-G) (the efficacy of Akt inhibition is indicated by the fact that Akt inhibitor V treatment abolished the phosphorylation of Akt in the liver tissues). Collectively, our findings support an important role of Akt in mPGES-1-mediated protection against Fas-induced liver injury.

Figure 5

A

B

C

D

E

F

G
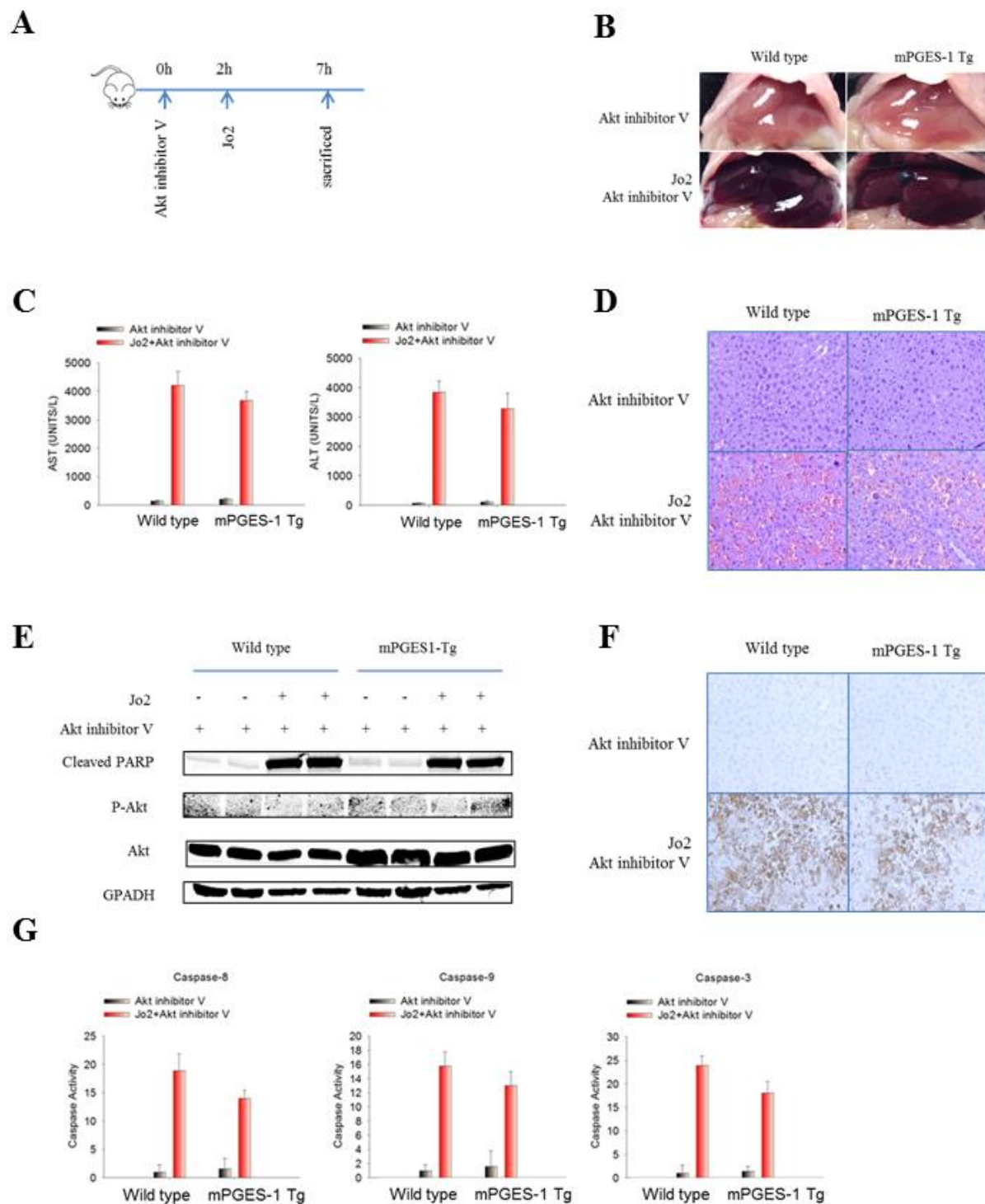
Figure 5. Akt inhibitor V restores the susceptibility of mPGES-1 Tg mice to Fas induced liver injury.

mPGES-1 Tg and their age/sex matched WT mice were intraperitoneally injected with a single dose of Akt inhibitor V (1µg/g body weight) 2h before Jo2 (0.5 ug/g body weight) injection. Mice were sacrificed at 5 h after Jo2 injection to collect serum and liver tissue samples.

(A) Timeline of the experiments. (B) Representative gross images of the livers from different groups of mice. (C) Serum ALT and AST levels. The data are expressed as mean±SE from three mice per group. (D) Representative microscopic images of the liver sections (H&E stain). (E) Western blotting for cleaved PARP, p-Akt and Akt in liver tissue homogenates. GAPDH was used as loading control. (F) Representative images of immunohistochemical stain for cleaved caspase-3 in liver tissues. (G) Caspase-9, 8, and 3 activities in liver tissue homogenates. The results are expressed as mean ± SE of fold changes over Akt inhibitor V-treated wild type group.

Figure 6
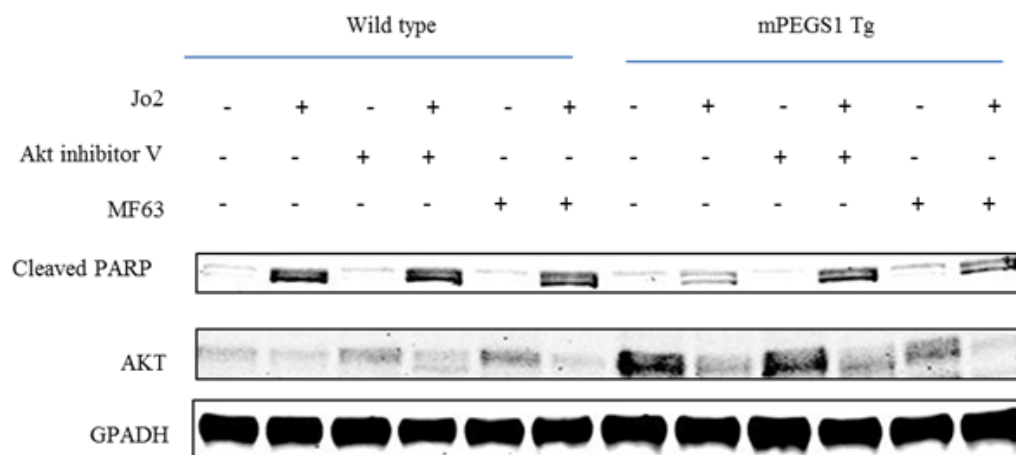
Figure 6. The levels of Akt and cleaved PARP.

Hepatocytes were isolated from wild type and mPGES-1 Tg mice and cultured in vitro. The cells were pretreated with the Akt inhibitor V (10µM) or MF63 (1µM) overnight. The pretreated cells were then challenged with Jo2 (0.2µg/ml) for 8h. The cell lysates were then obtained for Western blotting analysis to determine the protein levels of Akt and cleaved PARP. GAPDH was used as the loading control.

5. Discussion

In the current study, we developed a novel transgenic mouse model with targeted overexpression of mPGES-1 in the liver and the novel animals were utilized to assess Fas-induced hepatocyte apoptosis and acute liver injury. We observed that the mPGES-1 Tg mice were protected against Fas-induced hepatocyte apoptosis and liver injury (based on gross examination of the livers, histological evaluation of the liver tissues, assessment of serum transaminases levels, and caspase activity assays). These results are further corroborated by the finding that inhibition of mPGES-1 by its pharmacological inhibitor MF63 restored the susceptibility of mPGES-1 Tg mice to Jo2-induced liver injury.

Our findings suggest that hepatocyte mPGES-1 confers resistance to Fas-induced liver injury through activation of the Akt signaling cascade. This assertion is supported by the following observations: (1) under Jo2 treatment, the mPGES-1 Tg mice showed increased Akt activation as well as increased expression of Akt upstream activator (EGFR) and Akt downstream anti-apoptotic molecules (Mcl-1, Bcl-xl, p-Bad); (2) treatment of the mPGES-1 Tg mice with the mPGES-1 inhibitor MF63 reduced the level of Akt in hepatocytes and liver tissues; (3) treatment of mPGES-1 Tg mice with Akt inhibitor V restored the sensitivity of mPGES-1 Tg mice to Jo2-induced liver injury. Our data suggest mPGES-1-mediated upregulation of EGFR expression for activation of Akt and related anti-apoptotic molecules; this statement is consistent with the previous study that PGE_2 induces EGFR expression and Akt activation in hepatocytes [98].

PGE2 is known to play a proliferative and anti-apoptotic role in hepatocytes [99-101] and has been well documented to confer protection against liver damage in animal

experiments [102, 103]. Accordingly, transgenic mice with hepatic overexpression of COX-2 are resistant to Fas-induced liver injury [57, 104]. However, a limitation of the COX-2 transgenic mouse model relates to the fact that COX-2 mediates the synthesis of various prostanoids, including prostacyclin (PGI_2), thromboxane A_2 (TXA_2) and other prostanoids, in addition to PGE_2; as such, the possibility of contribution from other prostanoids could not be conclusively excluded for the COX-2 transgenic model. This drawback is avoided in the current study by liver-specific expression of mPGES-1, the terminal synthase of PGE_2.

In summary, this study describes a novel transgenic mouse model with targeted overexpression of mPGES-1 in the liver. We provide the first evidence that mPGES-1 overexpression in the liver prevents Fas-induced hepatocyte apoptosis and liver injury through activation of EGFR/Akt and downstream anti-apoptotic molecules. Further studies are warranted to evaluate whether induction of mPGES-1 expression or treatment with PGE_2 analogue could be developed as a new therapeutic strategy for effective prevention and treatment of Fas-associated liver injuries.

PART II. 15-hydroxyprostaglandin dehydrogenase (15-PGDH) prevents lipopolysaccharide (LPS)-induced acute liver injury

1. Liver specific expression of 15-PGDH protects mice from LPS/GalN-induced acute liver inflammation and tissue damage

We developed transgenic mice with targeted overexpression of 15-PGDH in the liver by microinjection of a construct containing the 15-PGDH transgene under the control of the albumin promoter/enhancer into fertilized mouse eggs of B6D2F1 mice at the single cell stage (illustrated in Figure 7). To determine the effect of hepatic 15-PGDH on endotoxin-induced liver injury, the 15-PGDH Tg mice and their age/sex matched wild type mice were intraperitoneally injected with a single dose of LPS/GalN and the animals were monitored over 24 hours. We observed prolonged survival of the 15-PGDH Tg mice (ranging from 8h to >24h, with 50% survival at 12.5h) compared to the wild type control mice (ranging from 5.5h to 10h, with 50% survival at 6.5h) (Figure 8A). Based on the survival curves, we sacrificed additional mice 5 hours after LPS/GalN injection, and the blood and liver tissues were collected to evaluate parameters of liver injury. The 15-PGDH transgenic mice had less prominent liver injury, as evidenced by lower serum ALT/AST levels (Figure 8B) and less hepatic necrosis/apoptosis (under H&E staining, caspase-3 immunostaining, and caspase activity assays, and PARP cleavage) (Figure 8C-E), compared to the wild type mice. We further observed that LPS/GalN treatment induced less hepatic inflammatory response in the 15-PGDH Tg mice, as reflected by the smaller population of F4/80 positive macrophages (Figure 8C) and the lower levels of

pro-inflammatory cytokines (Figure 8F, Figure 9), compared to the matched wild type mice.

Given that activation of JNK by TNFα is a predominant mechanism for hepatocyte apoptosis in LPS/GalN-induced liver injury [105, 106], we further measured the phosphorylation of JNK in the liver tissues. As shown in Figure 8E, overexpression of 15-PGDH in the liver completely prevented LPS/GalN-induced JNK phosphorylation. Taken together, these data provide novel evidence that the 15-PGDH Tg mice are resistant to LPS/GalN-induced acute liver inflammation/tissue damage.

Figure 7

A
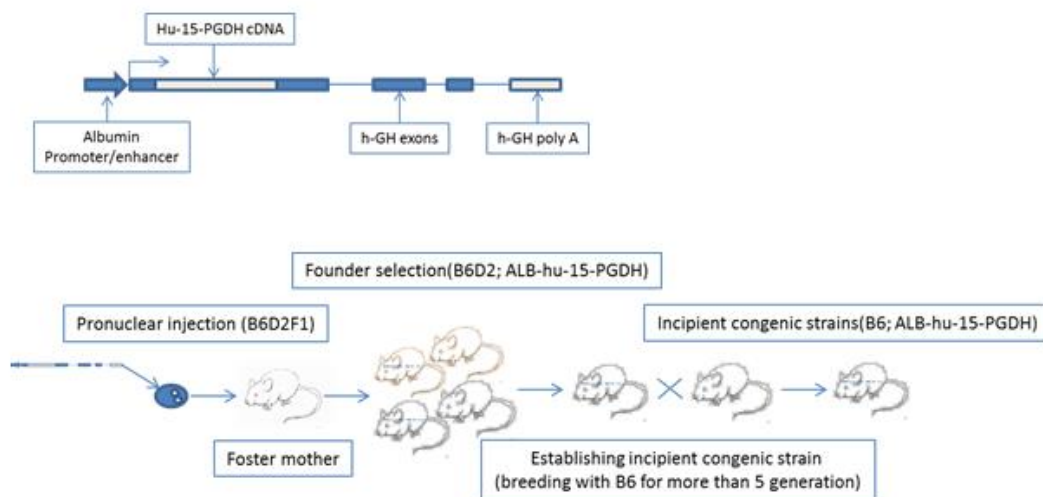
B
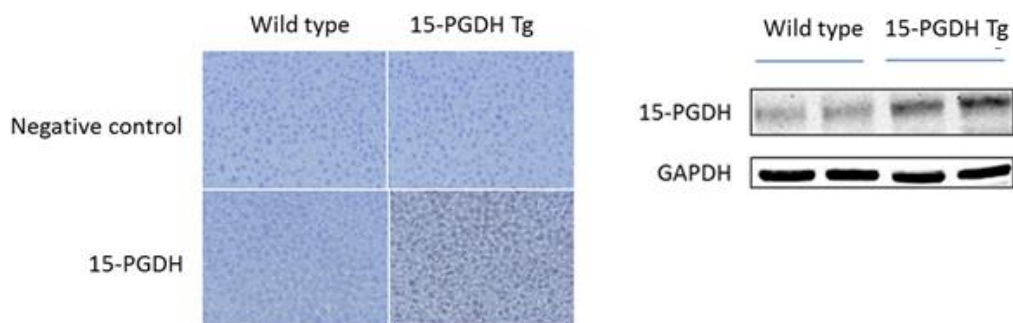
Figure 7. Development of liver specific 15-PGDH Tg mice.

(A) Schematic presentation of the strategy to develop 15-PGDH transgenic mice as described in the Methods. (B) The expression of 15-PGDH in liver tissues from wild type and Tg mice. (Left panel) Immunohistochemical stain for 15-PGDH in liver tissue

sections. (Right panel) 15-PGDH protein level in liver tissue homogenates (GAPDH as loading control).

Figure 8

A

B

C

D

E

F
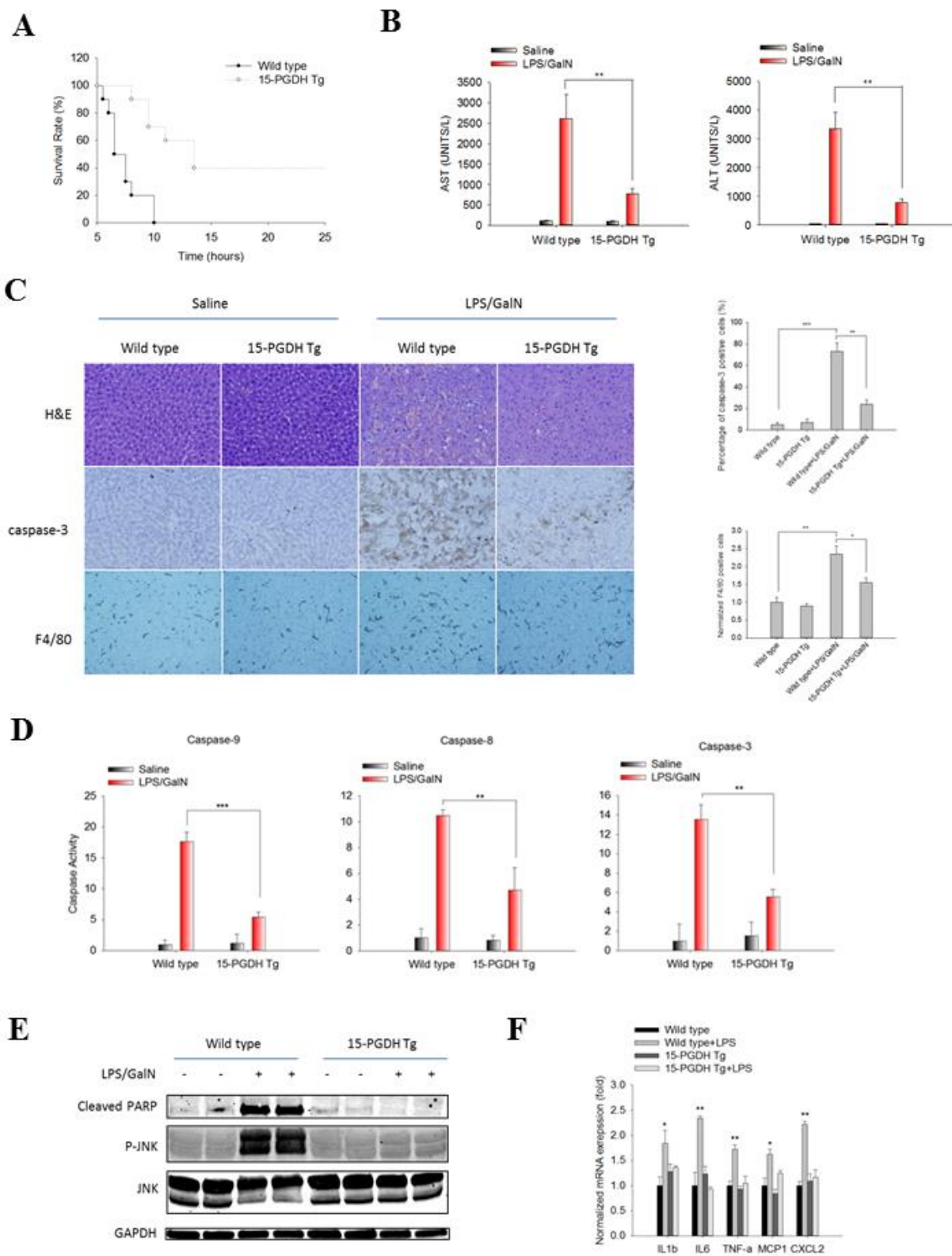
Figure 8. Liver specific 15-PGDH expression protects mice against LPS/GalN induced acute liver inflammation and tissue damage.

Wild type and 15-PGDH Tg mice were intraperitoneally injected with LPS/GalN (60ng/g, 800µg/g). The mice were followed for 24h for survival analysis or sacrificed at 5h after LPS/GalN injection to collect serum and liver tissue samples.

(A) Survival curve of mice after LPS/GalN administration. (B) Serum ALT and AST levels. The data are expressed as mean±SEM from three mice, ** $P<0.01$. (C) Representative images of liver tissue sections: H&E stain (upper panel), Caspase-3 immunostain (mid panel), F4/80 immunostain (lower panel). Quantified results are showed in the right panels (the data are expressed as mean±SEM from three mice, *$p<0.05$, **$p<0.01$, *** $P<0.001$). (D) Caspase-9, 8, and 3 activities in liver tissue homogenates. The results are presented as mean ± SEM of fold change relative to the saline-treated wild type group, *** $P<0.001$, **$p<0.01$. (E) The levels of apoptotic signaling molecules (Cleaved PARP, JNK, P-JNK) in liver tissue homogenates. GAPDH was used as loading control. (F) mRNA levels of pro-inflammatory cytokines (IL1ß, IL6, TNF-α, MCP1 and CXCL2) in liver tissue homogenates. The results are expressed as mean ± SEM of fold changes over wild type group (*$p<0.05$, **$p<0.01$ compared to 15-PGDH Tg+LPS group).

Figure 9
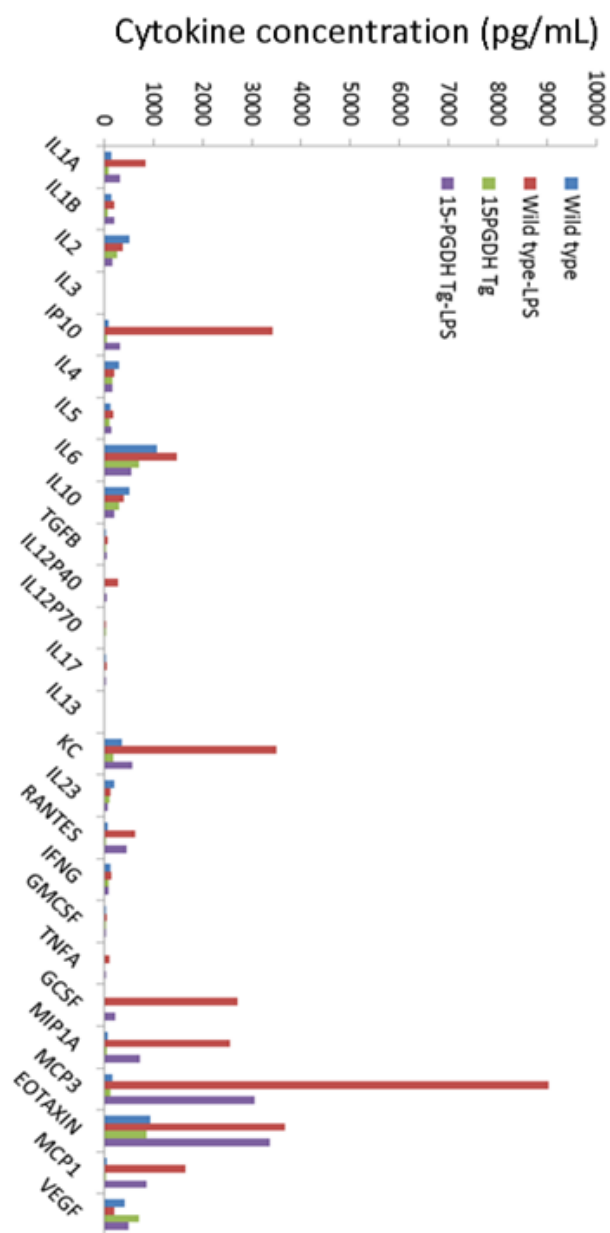
Figure 9. Cytokines levels in liver tissues.

Wild type and 15-PGDH Tg mice were intraperitoneally injected with LPS (60ng/g) plus GalN (800μg/g). The liver tissue samples were collected 5 hours after LPS/GalN injection. The levels of 26 cytokines in the liver tissue homogenates were analyzed as described in the Methods section.

2. Hepatic 15-PGDH expression indirectly influenced Kupffer cell activation

The pathological processes of LPS/GalN-induced acute liver injury are well-described, in which LPS initially activates Kupffer cells to release a variety of pro-inflammatory cytokines, chemokines and ROS; these mediators can directly induce hepatocyte damage or cause liver injury by activating other inflammatory cells [107]. Among the inflammatory mediators, TNFα is central in the development of liver injury, mainly through induction of hepatocyte apoptosis [105, 108]. To delineate the contribution of Kupffer cells and hepatocytes, we isolated Kupffer cells and hepatocytes from the 15-PGDH Tg mice and matched wild type mice. We first treated cultured Kupffer cells with LPS and observed that LPS treatment induced the expression of several pro-inflammatory cytokines, including TNFα, IL-1β, IL-6, MCP1 and CXCL2, in Kupffer cells from either wild type mice or 15-PGDH Tg mice (Figure 10A). Our data showed that the Kupffer cells isolated from wile type and 15-PGDH Tg mice responded similarly to LPS stimulation. We noted that 15-PGDH overexpression in hepatocytes did not significantly alter the expression of 15-PGDH in Kupffer cells (Figure 10A).

We next treated wild type or 15-PGDH-overexpressed hepatocytes with TNF-α (a predominant inflammatory cytokine released by Kupffer cells in response to LPS stimulation). Our data showed that the hepatocytes isolated from wild type and 15-PGDH Tg mice had a similar degree of JNK activation, ROS production and apoptosis in response to TNF-α treatment (Figure 10B-D). Therefore, 15-PGDH expression in hepatocytes does not significantly alter their response to TNF-α.

To investigate the possible interaction between hepatocytes and Kupffer cells, we treated wild type Kupffer cells with the conditioned medium (CM) derived from wild type or 15-PGDH-Tg hepatocytes, and the Kupffer cell primed by the hepatocyte CM were then utilized to determine their response to LPS. We observed that the wild type Kupffer cells pre-incubated with the CM from 15-PGDH-Tg hepatocytes had less cytokine expression in response to LPS stimulation (compared to Kupffer cells pre-incubated with the CM from wild type hepatocytes) (Figure 10E). These findings suggest that 15-PGDH in hepatocytes may regulate the production of soluble mediators which indirectly impact Kupffer cell response to LPS.

Figure 10
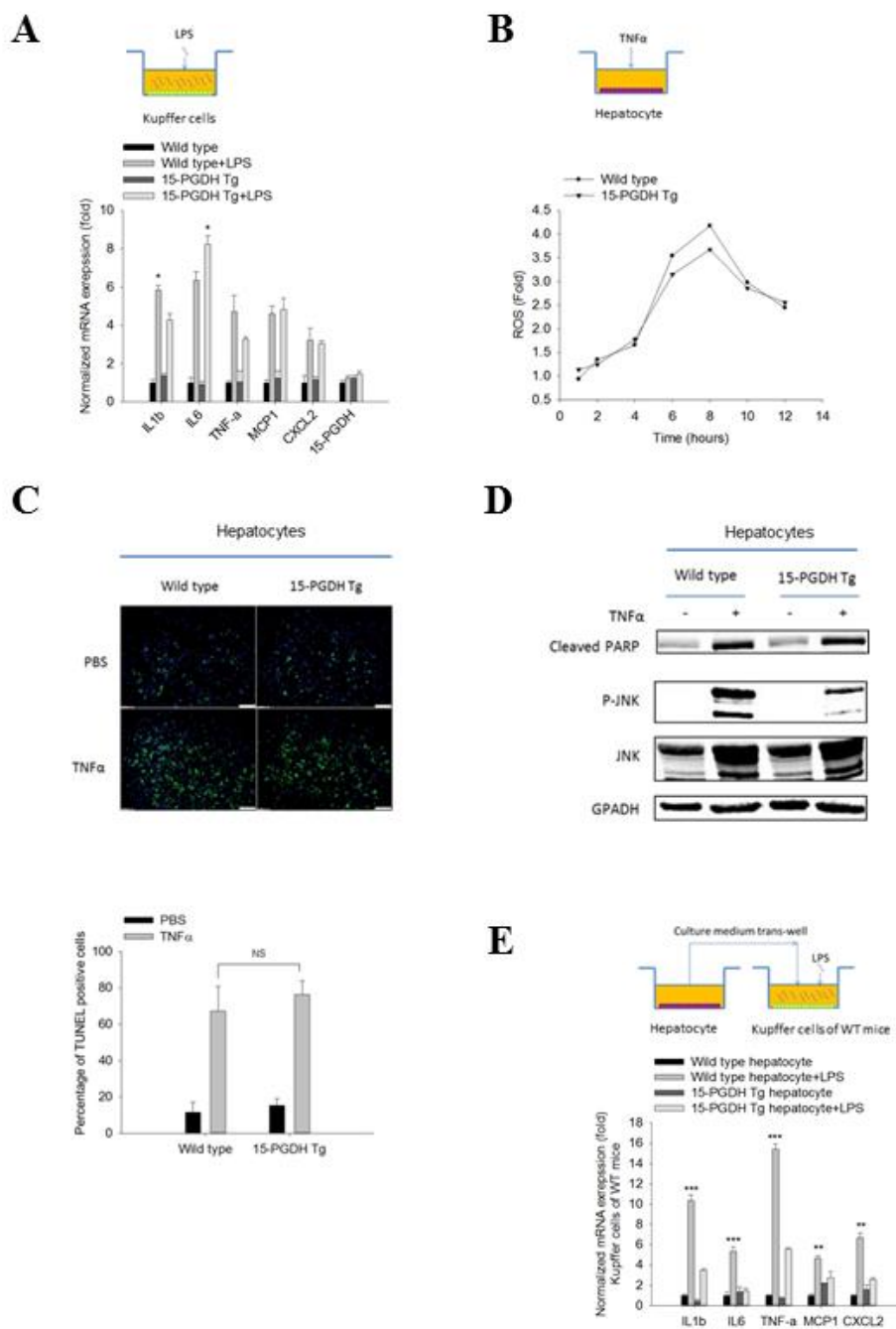
Figure 10. 15-PGDH expression in hepatocytes regulates Kupffer cell cytokine production.

Kupffer cells and hepatocytes were isolated and cultured separately. LPS (10ng/ml) was used to elicit Kupffer cell inflammatory response. TNF-α (25 ng/ml) plus ActD (0.4 µg/ml) was used to induce hepatocyte apoptosis.

(A) mRNA level of pro-inflammatory cytokines (IL1ß, IL6, TNF-α, MCP1 and CXCL2) and 15-PGDH in Kupffer cells after LPS treatment (6h). The results are expressed as mean ± SEM of fold changes over wild type group (*p<0.05, **p<0.01 compared to 15-PGDH Tg+LPS group). (B) Accumulation of reactive oxygen species (ROS) in hepatocytes after TNF-α treatment. ROS was measured by dichlorofluorescin fluorescence assay and expressed as fold change over 0h time point. (C) Hepatocyte apoptosis induced by TNF-α treatment (8h). Apoptotic hepatocytes were stained by TUNEL assay. Representative images are showed in the upper panel. Quantified results are showed in the lower panel (NS, no statistical significance). (D) The levels of apoptotic signaling molecules (Cleaved PARP, JNK, P-JNK) in hepatocytes after LPS treatment (8h). GAPDH was used as loading control. (E) mRNA levels of pro-inflammatory cytokines (IL1b, IL6, TNF-α, MCP1 and CXCL2) in WT Kupffer cells treated with hepatocyte CM followed by LPS. The results are expressed as mean ± SE of fold changes over wild type hepatocyte group. (**p<0.01, ***p<0.001 compared to 15-PGDH Tg hepatocyte+LPS group).

3. 15-PGDH-derived 15-keto-PGE$_2$ from hepatocytes inhibits Kupffer cell activation via PPAR-γ

15-PGDH is well noted as the enzyme catalyzing conversion of pro-inflammatory PGE$_2$ to its oxidized product, 15-keto-PGE$_2$, which is an endogenous PPAR-γ ligand [11, 12]. Notably, PPAR-γ is a pivotal nuclear receptor that negatively regulates the production of pro-inflammatory cytokines in Kupffer cells [109]. Thus, we postulated that the 15-PGDH-derived 15-keto-PGE$_2$ in hepatocytes may regulate Kupffer cell activation via PPAR-γ through a paracrine mechanism. In support of this, we observed significantly increased 15-keto-PGE$_2$ production by 15-PGDH-Tg hepatocytes compared to the wild type hepatocytes (especially when the cells were supplemented with the prostaglandin substrate, arachidonic acid (AA) (Figure 11A). The observation that 15-PGDH inhibitor decreased 15-keto-PGE$_2$ production in 15-PGDH Tg hepatocytes further support the role of 15-PGDH for 15-keto-PGE$_2$ production. To further determine the impact of 15-keto-PGE$_2$ on Kupffer cells, we pre-treated Kupffer cells with 15-keto-PGE$_2$ prior to LPS stimulation. Our data showed that 15-keto-PGE$_2$ treatment significantly inhibited LPS-induced cytokine expression in Kupffer cells (Figure 11B, Figure 12A-B). We observed that the effect of 15-keto-PGE$_2$ on Kupffer cell inhibition was as potent as the conditioned medium from 15-PGDH-Tg hepatocytes. These findings strongly support hepatocyte-derived 15-keto-PGE$_2$ for inhibition of Kupffer cell activation.

We sought to further determine the role of PPAR-γ in this process, and found that treatment of wild type Kupffer cells with 15-keto-PGE$_2$ or the conditioned medium (CM)

of 15-PGDH Tg hepatocytes increased the expression of the PPAR-γ down-stream genes (CD36, ADRP, CPT1a, ABCG1) (Figure 11C). To determine whether 15-keto-PGE$_2$ or 15-PGDH Tg hepatocyte CM might alter PPAR-γ protein binding to its DNA response element, we performed gel electrophoresis mobility shift assay (EMSA) in a mouse macrophage cell line (RAW264.7) using an oligonucleotide corresponding to PPRE (PPAR response element). We observed that treatment of RAW264.7 cells with 15-keto-PGE$_2$ or 15-PGDH Tg hepatocyte CM enhanced binding to PPRE (Figure 11D). These findings support the notion that 15-PGDH-derived 15-keto-PGE$_2$ from hepatocytes can activate PPAR-γ in macrophages. The latter assertion is further supported by the observation that the PPAR-γ antagonist, GW9662, reversed Kupffer cell inhibition by 15-keto-PGE$_2$ and by 15-PGDH Tg hepatocyte CM (Figure 11E, Figure 12C). Together, our results suggest that 15-PGDH-derived 15-keto-PGE$_2$ from hepatocytes inhibited Kupffer cell activation by binding to PPAR-γ and that this mechanism may explain the resistance of 15-PGDH Tg mice to LPS/GalN induced liver injury.

Figure 11
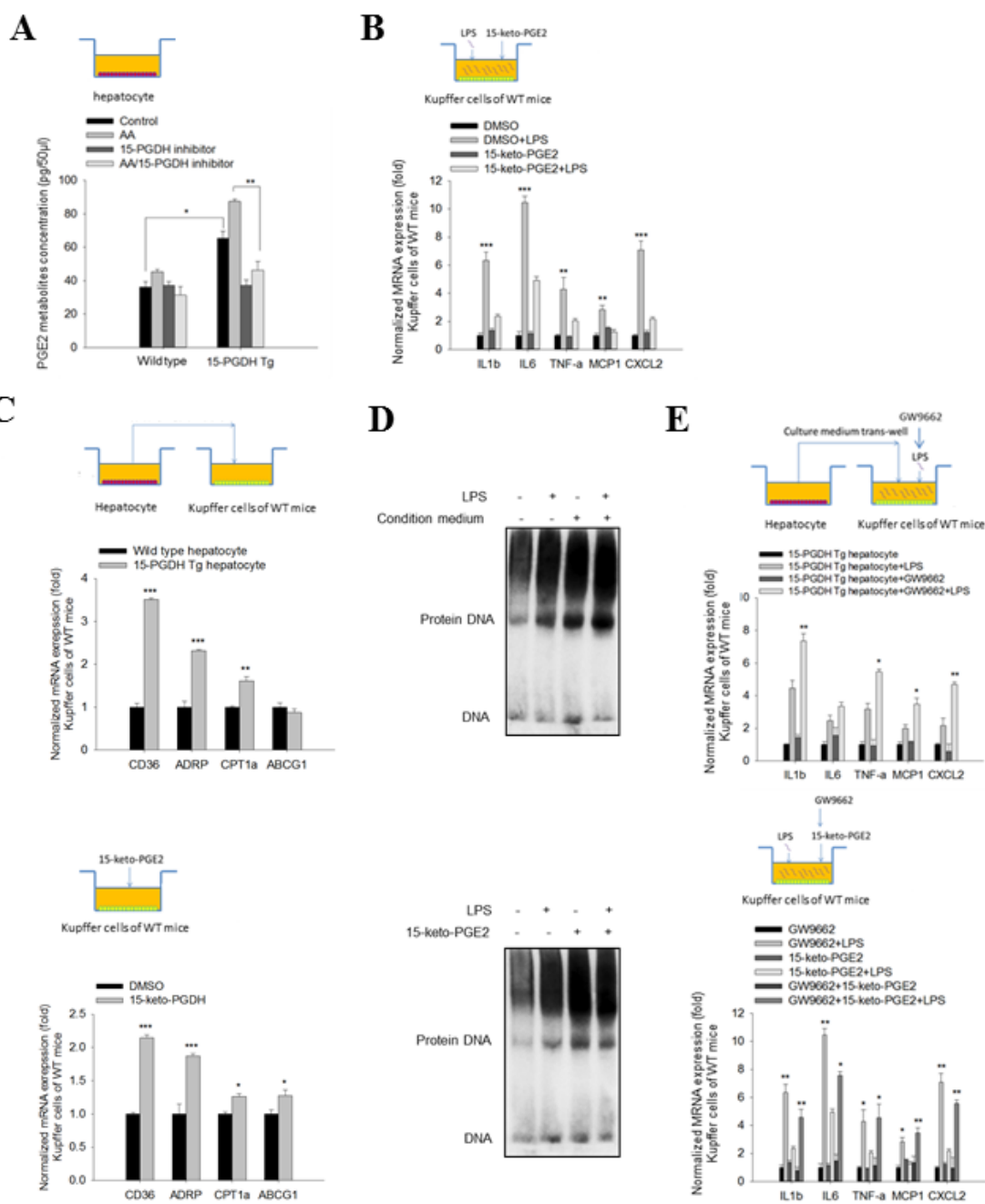
Figure 11. 15-PGDH-derived 15-keto-PGE$_2$ from hepatocytes inhibits Kupffer cell activation via PPAR-γ

(A) Concentration of PGE$_2$ metabolites in hepatocyte CM as measured by the Prostaglandin E Metabolite assay. We observed that 15-PGDH overexpression enhanced PGE$_2$ metabolite production and this effect was more apparent in the presence of arachidonic acid substrate (10μM); this effect was blocked by treatment with the 15-PGDH inhibitor (1μM). The data are expressed as mean±SE, *p<0.05, **p<0.01. (B) mRNA levels of pro-inflammatory cytokines (IL1ß, IL6, TNF-α, MCP1 and CXCL2) in WT Kupffer cells treated with 15-keto-PGE$_2$ (10μM) followed by LPS. The results are expressed as mean ± SE of fold changes over DMSO group (**p<0.01, ***p<0.001 compared to 15-keto-PGE$_2$+LPS group). (C) mRNA levels of PPAR-γ downstream genes (CD36, ADRP, CPT1α and ABCG1) in WT Kupffer cells treated with hepatocyte CM (upper panel) or 15-keto-PGE$_2$ (10μM) (lower panel). The data are expressed as mean±SEM of fold changes (*p<0.05, **p<0.01, ***P<0.001). (D) DNA binding ability of PPAR-γ from mouse macrophages (RAW264.7) treated with hepatocyte CM (upper panel) or 15-keto-PGE2 (10μM) (lower panel), as determined by EMSA assay using PPRE dsDNA. (E) mRNA levels of pro-inflammatory cytokines (IL1ß, IL6, TNF-α, MCP1 and CXCL2) in WT Kupffer cells treated with hepatocyte CM (upper panel) or 15-keto-PGE$_2$ (10μM) (lower panel) (with or without GW9662 [10μM] or LPS treatment). For the upper panel, the results are expressed as mean ± SE of fold changes over 15-PGDH Tg hepatocyte group (*p<0.05, **p<0.01 compared to 15-PGDH Tg hepatocyte+LPS group). For the lower panel, the results are expressed as mean ± SEM of

fold changes over GW9662 group (*p<0.05, **p<0.01 compared to 15-keto-PGE$_2$+LPS group).

Figure 12
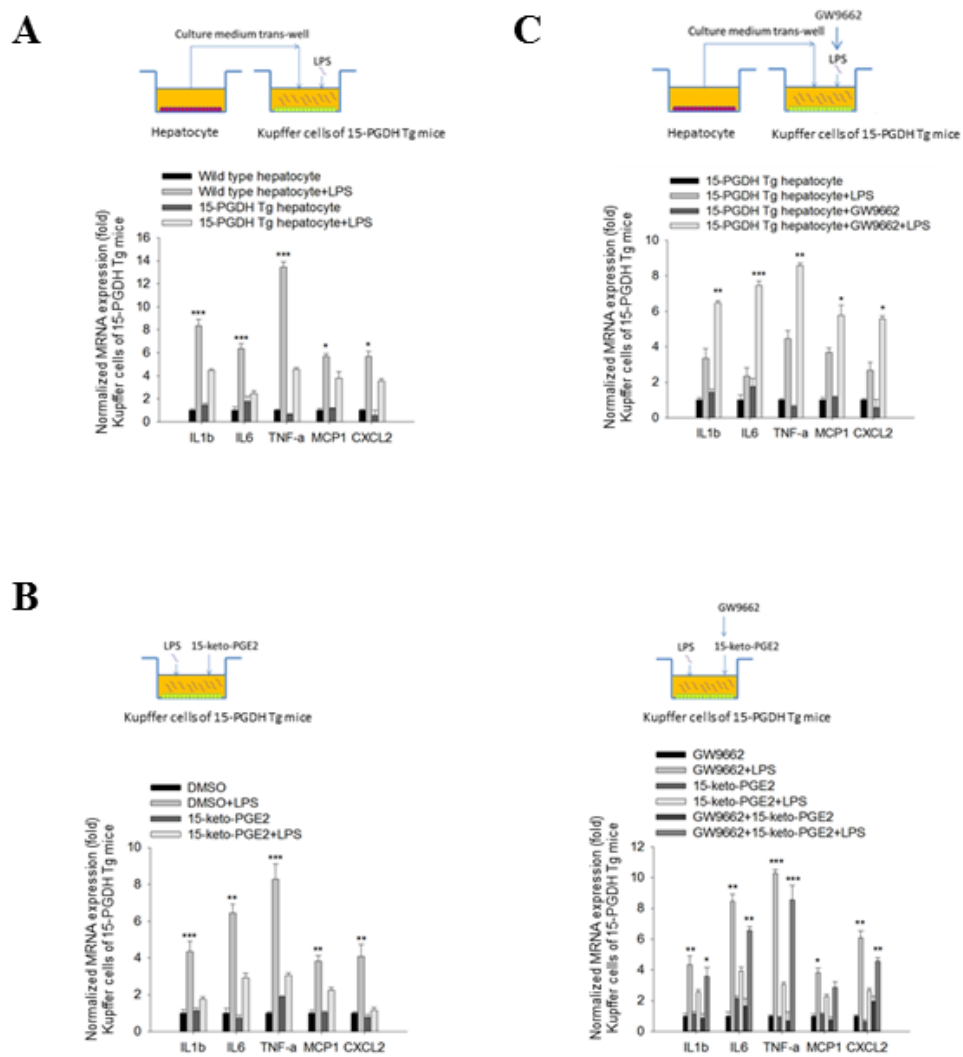
Figure 12. 15-PGDH-derived 15-keto-PGE$_2$ from hepatocytes inhibits Kupffer cell inflammatory response via PPAR-γ.

(A) mRNA levels of pro-inflammatory cytokines (IL1ß, IL6, TNF-α, MCP1 and CXCL2) in Kupffer cells isolated from the 15-PGDH Tg mice. The Kupffer cells were treated with the indicated hepatocyte CM followed by LPS. The results are expressed as mean ± SE of fold changes over wild type hepatocyte group (*p<0.05, ***p<0.001 compared to 15-PGDH Tg hepatocyte+LPS group). (B) mRNA levels of pro-inflammatory cytokines (IL1ß, IL6, TNF-α, MCP1 and CXCL2) in Kupffer cells isolated from the 15-PGDH Tg mice. The Kupffer cells were treated with 15-keto-PGE$_2$ (10µM) followed by LPS. The results are expressed as mean ± SEM of fold changes over DMSO group (**p<0.01, ***p<0.001 compared to 15-keto-PGE$_2$+LPS group). (C) mRNA levels of pro-inflammatory cytokines in Kupffer cells isolated from the 15-PGDH Tg mice. The Kupffer cells were treated with the indicated hepatocyte CM (upper panel) or 15-keto-PGE$_2$ (10µM) (lower panel) with or without GW9662 (10µM) or LPS. For the upper panel, the results are expressed as mean ± SEM of fold changes over 15-PGED Tg hepatocyte group (*p<0.05, **p<0.0, ***p<0.001 compared to 15-PGDH Tg hepatocyte+LPS group). For the lower panel, the results are expressed as mean ± SE of fold changes over GW9662 group (*p<0.05, **p<0.01, ***p<0.001 compared to 15-keto-PGE$_2$+LPS group).

4. PPAR-γ antagonist restored 15-PGDH Tg mice susceptibility to LPS/GalN induced acute liver inflammation and tissue damage

To further verify the role of PPAR-γ, we administered the PPAR-γ antagonist, GW9662, to 15-PGDH Tg mice prior to LPS/GalN administration. We observed that GW9662 pretreatment reversed the resistance of 15-PGDH Tg mice to LPS/GalN-induced acute liver injury. As shown in Figure 13A-B, LPS/GalN-induced an increase of serum ALT/AST and hepatocyte necrosis/apoptosis were comparable between the GW9662 pretreated 15-PGDH Tg mice and wild type mice. Likewise, the LPS/GalN-induced JNK phosphorylation, PARP cleavage and activation of Caspase3/8/9 were also comparable between the GW9662 pretreated 15-PGDH Tg mice and wild type mice (Figure 13C-D). Our data showed that GW9662 pretreatment of 15-PGDH Tg mice restored their susceptibility to LPS/GalN induced acute liver inflammation (as reflected by macrophage populations and cytokine levels) (Figure 13B, 13E). Collectively, these findings demonstrate that inhibition of PPAR-γ by its antagonist GW9662 can restore the susceptibility of the 15-PGDH Tg mice to LPS/GalN induced acute liver inflammation/injury.

Figure 13
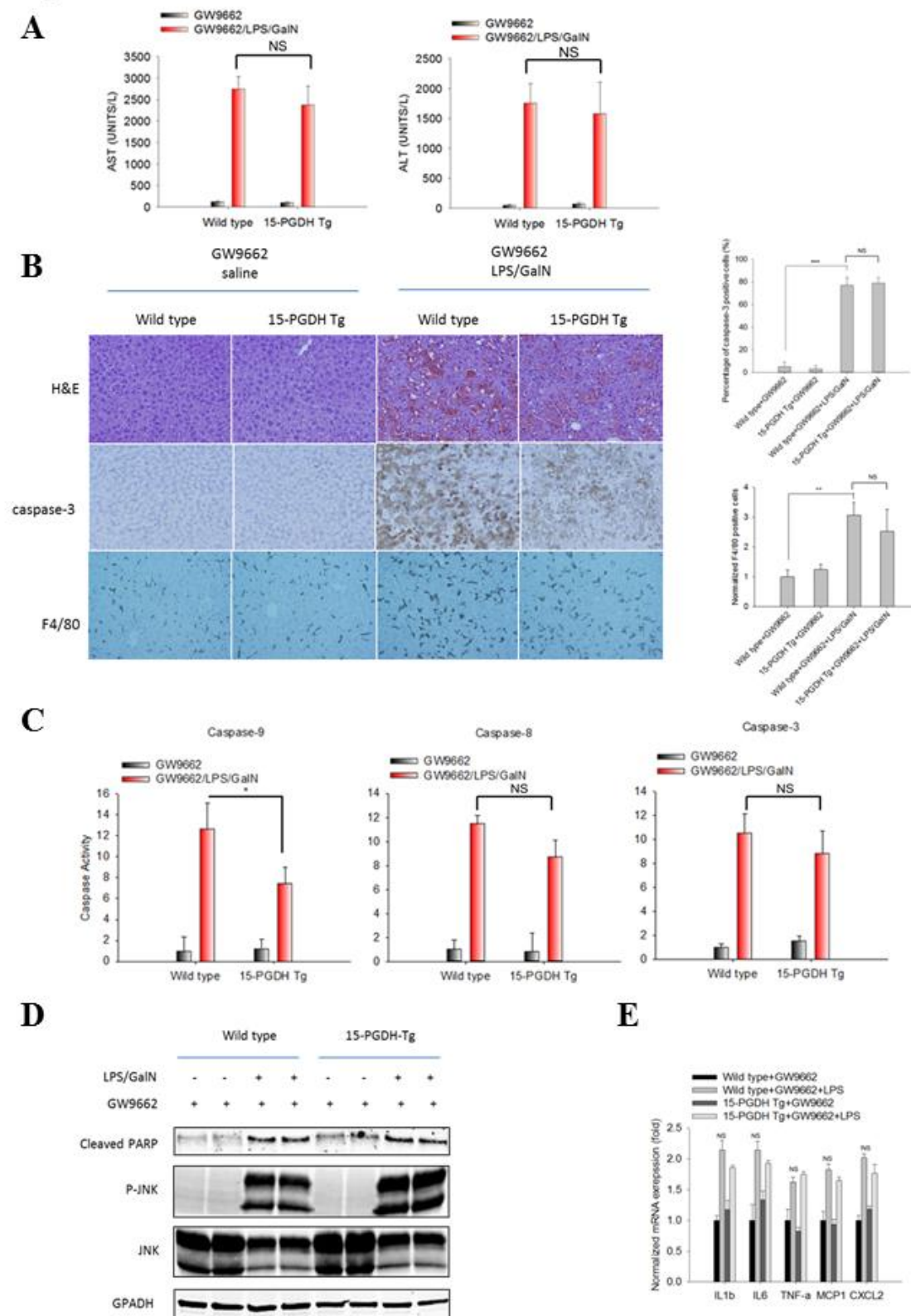
Figure 13. PPAR-γ antagonist restores the susceptibility of the 15-PGDH Tg mice to LPS/GalN-induced acute liver inflammation/injury.

Wild type and 15-PGDH Tg mice were intraperitoneally injected with GW9662 (1µg/g) 2h before LPS/GalN administration. Mice were sacrificed 5 hours after LPS/GalN injection to collect serum and liver tissue samples.

(A) Serum ALT and AST levels. The data are expressed as mean±SE from three mice (NS, no statistical significance). (B) Representative images of liver tissue sections: H&E stain (upper panel), caspase-3 immunostain (mid panel), F4/80 immunostain (lower panel). Quantified results are showed at the right panels (the data are expressed as mean±SE from three mice; **p<0.01, *** P<0.001, NS - no statistical significance). (C) Caspase-9, 8, and 3 activities in liver tissue homogenates. The results are presented as mean ± SE of fold changes over GW9662-treated wild type group (NS, no statistical significance). (D) The levels of apoptotic signaling molecules (Cleaved PARP, JNK, P-JNK) in liver tissue homogenates. GAPDH was used as loading control. (E) mRNA levels of pro-inflammatory cytokines (IL1ß, IL6, TNF-α, MCP1 and CXCL2) in liver tissue homogenates. The results are expressed as mean ± SE of fold changes over wild type+GW9662 group (NS, no statistical significance compared to 15-PGDH Tg+GW9662+LPS group).

5. Discussion

15-PGDH is known to catalyze the oxidation of PGE_2, a potent pro-inflammatory and pro-proliferative lipid mediator, to 15-keto-PGE_2. While 15-keto-PGE_2 had been long considered as an inactive metabolite of PGE_2, recent studies have shown that 15-keto-PGE_2 is biologically active by serving as an endogenous PPAR-γ ligand. The current study provides novel evidence that 15-keto-PGE_2 signaling via PPAR-γ has an anti-inflammatory property in the setting of endotoxin-associated liver inflammation/injury. We show that after LPS/D-GalN injection, the 15-PGDH Tg mice exhibit much less necro-inflammatory response and less liver tissue damage compared to the wild type mice. This phenomenon is explained by the fact that 15-PGDH-derived 15-keto-PGE_2 from hepatocytes is able to inhibit LPS-induced cytokine production in Kupffer cells, as depicted in the current study.

Our findings suggest that 15-PGDH-derived 15-keto-PGE_2 from hepatocytes attenuates endotoxin-induced liver inflammation/injury via activation of PPAR-γ in Kupffer cells. This assertion is consistent with the previous studies documenting an anti-inflammatory effect of PPAR-γ in Kupffer cells (where PPAR-γ inhibits the production of inflammatory cytokines). In this context, it is worth mentioning that PPAR-γ has been well documented to inhibit the expression of pro-inflammatory genes in macrophages [110, 111]. Our data presented in the current study are also consistent with a recent in vivo study showing that mice with targeted deletion of PPAR-γ in Kupffer cells developed an exacerbated response to CCl4-induced liver injury (characterized by higher necro-inflammatory activity, more prominent liver tissue injury and aggravated fibrogenic response). In our system, we show that 15-keto-PGE_2 is able to activate

PPAR-γ in mouse macrophages, as indicated by the fact that 15-keto-PGE$_2$ enhances the DNA binding ability of PPAR-γ and induces the expression of PPAR-γ down-stream genes. Further, our data indicate that the PPAR-γ antagonist, GW9662, is able to reverse 15-keto-PGE$_2$-induced inhibition of cytokine production in Kupffer cells in vitro and can also restore the susceptibility of 15-PGDH Tg mice to LPS/GalN-induced liver injury in vivo. Taken together, these findings disclose a novel interaction between 15-PGDH/15-keto-PGE$_2$ in hepatocytes and PPAR-γ signaling in Kupffer cells which coordinately regulate endotoxin-associated liver inflammation/injury.

In essence, the current study demonstrates that hepatic 15-PGDH protects against endotoxin-induced acute liver injury. Our findings point toward the possibility of 15-PGDH induction or 15-keto-PGE$_2$ analogue as potential therapy for the treatment of inflammation-associated liver injury. In this context, it is notable that Zhang and colleagues [25] recently described that 15-PGDH negatively regulates liver and colon tissue regeneration; the authors suggest that 15-PGDH inhibition may represent a therapeutic strategy to enhance tissue repair after injury in diverse clinical contexts. However, their findings are in contrast with our results presented in the current study which show that 15-PGDH in the liver actually reduces endotoxin-mediated inflammation and prevents liver tissue injury. Our data suggest that induction, rather than inhibition, of 15-PGDH may have therapeutic value for the treatment of inflammation-associated liver injury. This viewpoint is of critical importance, given that inflammation-associated tissue injury and repair is pivotal in the pathogenesis of liver diseases associated with various underlying causes. Thus, concern exists on the proposed 15-PGDH inhibition for tissue regeneration in diverse clinical contexts [25, 112],

considering that 15-PGDH inhibition may exacerbate liver necro-inflammatory response and such a drawback could outweigh the perceived benefits of enhancing tissue regeneration. Consequently, whether 15-PGDH ought to be induced or inhibited for therapy is context-dependent and requires careful consideration of the underlying liver diseases.

PART III. Omega-3 Polyunsaturated Fatty Acids Upregulate 15-PGDH Expression in Cholangiocarcinoma Cells by Inhibiting miR-26a/b Expression

1. ω-3 PUFAs induces 15-PGDH expression in human cholangiocarcinoma cells

We compared the effect of w-3 PUFA (DHA) versus w-6 PUFA (AA) on 15-PGDH expression in human cholangiocarcinoma cell lines (CCLP1 and TFK-1). Although DHA treatment increased the level of 15-PGDH protein, AA treatment exhibited no effect (Figure 14A and Figure 15). In separate experiments, we stably transfected CCLP1 and TFK-1 cells with vector expressing the Fat-1 gene (which encodes a C. elegans w-3 fatty-acid desaturase converting w-6 to w-3 fatty acids; [113]). Overexpression of the Fat-1 gene was also found to increase 15-PGDH protein expression; the effect of Fat-1 gene transfection on 15-PGDH is comparable with DHA treatment of control cells (Figure. 14B). In addition, the levels of 15-PGDH mRNA were also elevated in DHA-treated or Fat-1–overexpressed cells (Figure. 14C). DHA treatment or Fat-1 expression did not alter 15-PGDH promoter activity, as reflected by the 15-PGDH promoter luciferase assay (Figure. 14D).

Figure 14
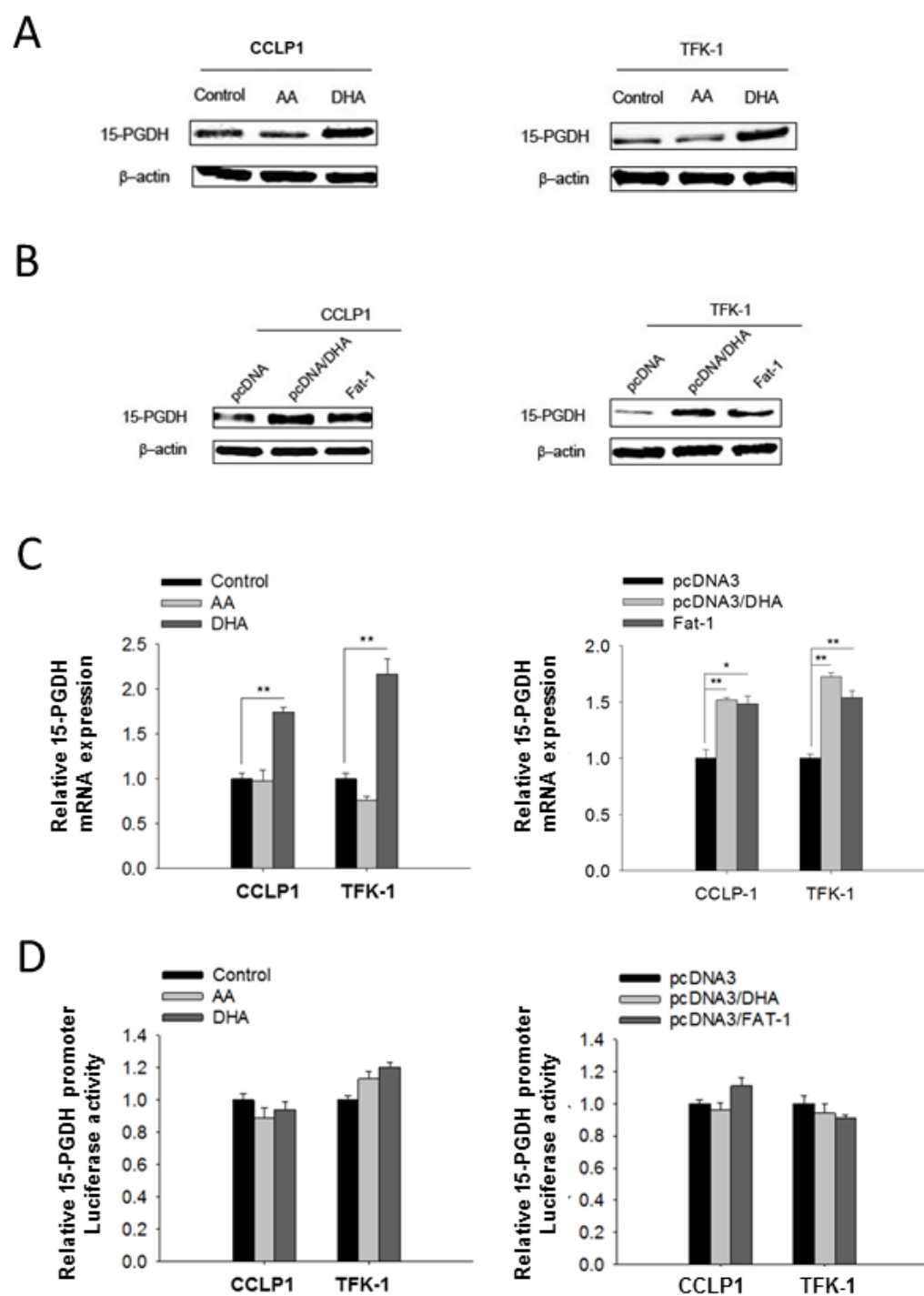
Figure 14. ω-3 PUFAs induces 15-PGDH expression in human cholangiocarcinoma cells.

(A) 15-PGDH protein level increased in cholangiocarcinoma cells cultured with ω-3 PUFA DHA but not with ω-6 PUFA AA. CCLP1 or TFK-1 cells were synchronized by serum deprivation, and then maintained in serum-free medium containing 50 μM DHA or AA for 12 h; (B) 15-PGDH protein level increased in cholangiocarcinoma cells expressing Fat-1 which converts ω-6 PUFA to ω-3 PUFA. CCLP1 or TFK-1 cells stably transfected with Fat-1 expression vector or control vector were synchronized by serum deprivation. The cells were treated with or without 50 μM DHA in serum-free medium for 12 h. Total protein was analyzed by Western blotting with 15-PGDH antibody. β-actin was measured as a reference gene. (C) DHA treatment or Fat-1 gene expression increases 15-PGDH mRNA levels in cholangiocarcinoma cells. 15-PGDH mRNA was measured by real-time PCR. Results were normalized to control group; the data are shown with mean±SE. $*P<0.05$, $**P<0.01$; (D) 15-PGDH promoter activity was not influenced by DHA treatment or Fat-1 expression in cholangiocarcinoma cells. CCLP1 or TFK-1 cells were co-transfected with 15-PGDH promoter-luc3 and pRL-TK plasmid which encodes Renilla luciferase. 72h after transfection, Luciferase activity was measured. Results were normalized to control group. Data were shown with mean±SE.

Figure 15
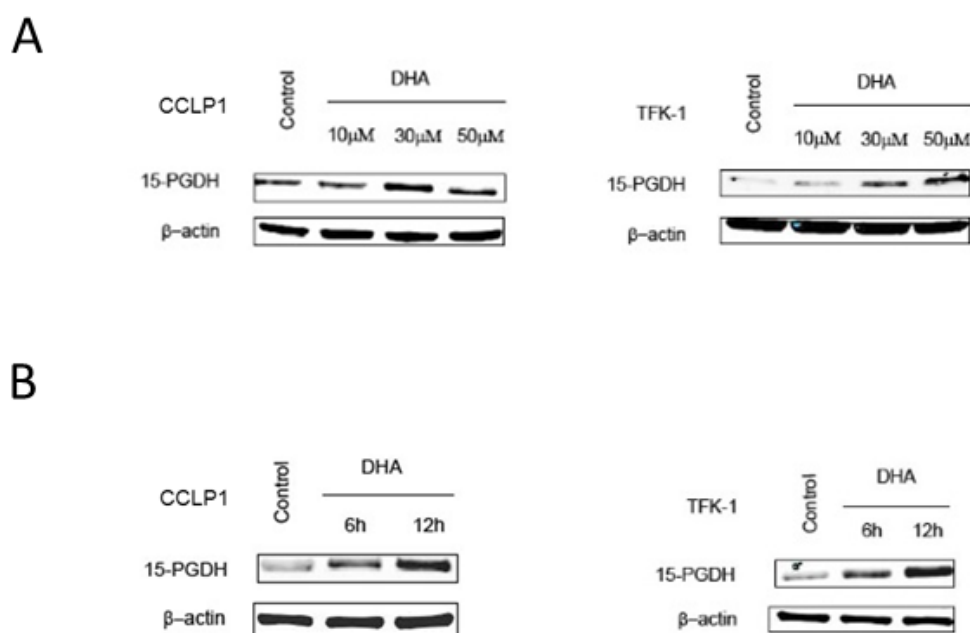
Figure 15. ω-3 PUFAs induce 15-PGDH expression in human cholangiocarcinoma cells.

(A) 15-PGDH expression in CCLP1 and TFK-1 cells treated with DHA at different doses. (B) 15-PGDH expression in CCLP1 and TFK-1 cells treated with 50 μM DHA for different time periods.

2. ω-3 PUFAs suppress miR-26a/b and prevent their targeting of 15-PGDH in cholangiocarcinoma cells

As ω-3 PUFA increased 15-PGDH protein and mRNA level without induction of 15-PGDH promoter activity, we reasoned that w-3 PUFA might regulate 15-PGDH gene expression through a posttranscriptional mechanism. We directed our attention to microRNAs, which could potentially bind to the 15-PGDH 3'UTR. Sequence analysis identified four conserved microRNAs (miR-26a, miR-26b, miR-1297, and miR-4465) that are complementary to the 15-PGDH 3'UTR (Figure 16A and Figure 17). Among these four microRNAs, miR-26a and miR-26b were found to be highly expressed in cholangiocarcinoma cells relative to the other two (miR-1297 and miR-4465; Figure 17). We next performed qRT-PCR analysis to determine whether ω-3 PUFAs might alter the expression of these miRNAs. As shown in Figure 16B and C, DHA treatment or Fat-1 overexpression decreased the levels of miR-26a and miR-26b, but not the other two miRNAs (miR-1297 and miR-4465). These findings suggest that ω-3 PUFA may induce 15-PGDH expression through alteration of miR-26a and/or miR-26b.

To further determine the effect of miR-26a and miR-26b on 15-PGDH, we infected human cholangiocarcinoma cells with lentivirus particles carrying the miR-26a (green) or miR-26b gene (red; Figure 16D); these cells were then analyzed for 15-PGDH protein expression. As shown in Figure 16E, overexpression of miR-26a or miR-26b significantly reduced 15-PGDH protein in both CCLP1 and TFK-1 cells and the effects were reversed by antimiR-26. We next measured the 15-PGDH 3'UTR luciferase reporter activities in miR-26a or miR-26b overexpressed or control cells. As shown in Figure 16F, miR-26a or miR-26b overexpression decreased the 15-PGDH 3'UTR luciferase reporter

activity; this effect was abolished when the miR-26a/b–binding sites were mutated. These results establish 15-PGDH as a direct target of miR-26a/b. Accordingly, we observed that overexpression of miR-26a or miR-26b prevented DHA-induced 15-PGDH protein accumulation (Figure 16G).

Taken together, our findings suggest that w-3 PUFAs induce 15-PGDH protein accumulation through suppression of miR-26a/b in human cholangiocarcinoma cells.

Figure 16
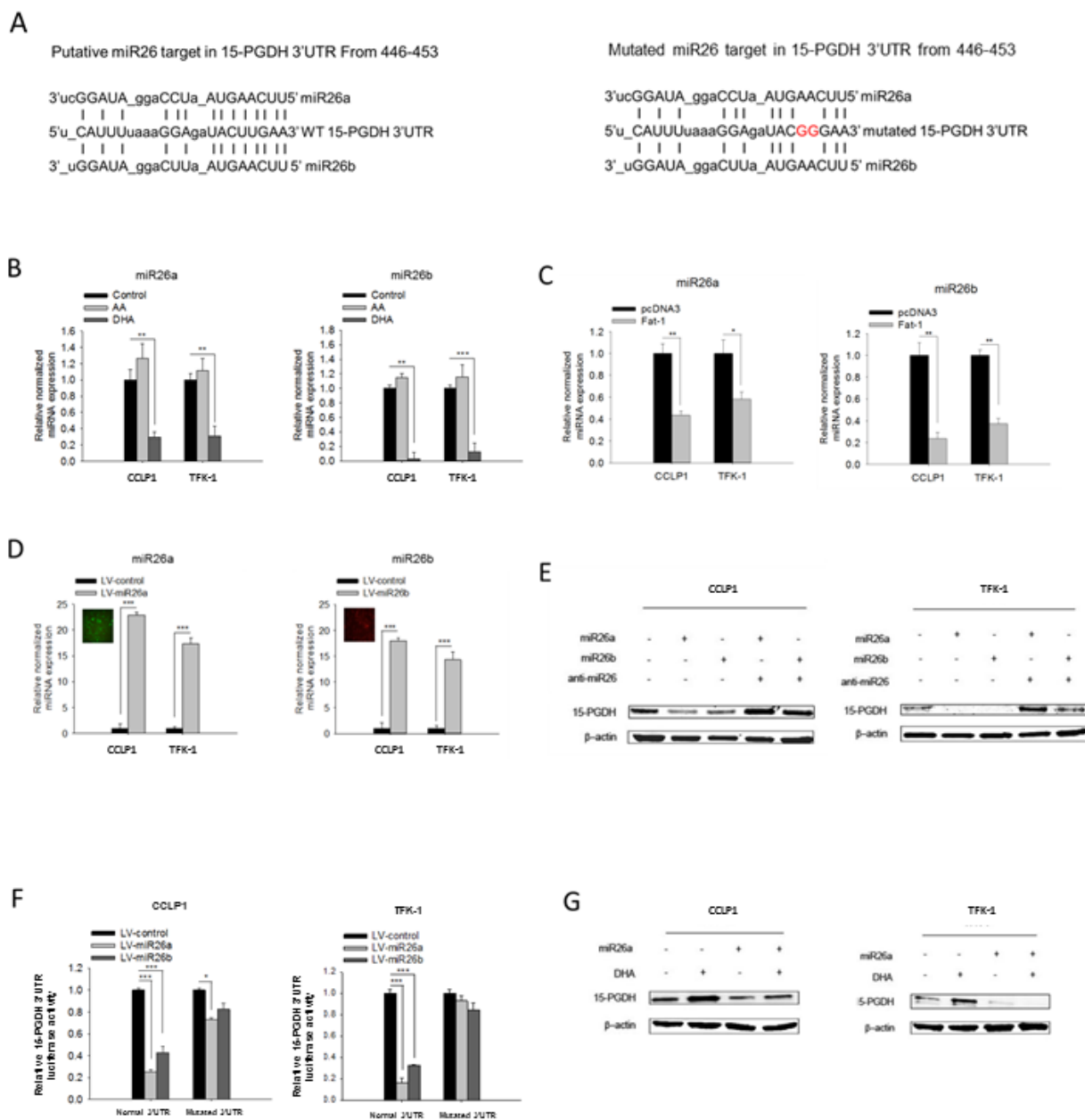
Figure 16. ω-3 PUFAs suppress miR26a/b and prevent their targeting of 15-PGDH in cholangiocarcinoma cells.

(A) Putative miR26a and miR26b binding site in normal 3′-UTR or mutated 3′-UTR of 15-PGDH mRNA. (B) DHA, but not AA, decreases the levels of miR26a and miR26b in cholangiocarcinoma cells. CCLP1 or TFK-1cells were synchronized by serum deprivation, and then maintained in serum-free medium containing 50 μM DHA or AA for 12 h; (C) Fat-1 expression decreased miR26a and miR26b levels in cholangiocarcinoma cells. (D) The levels of miR26a or miR26b in cholangiocarcinoma cells infected with respective lentiviral vectors. CCLP1 or TFK-1 cells were infected with miR26a or miR26b lentivirus and then subjected to Geneticin selection. miR26a and miR26b were measured by real-time PCR. Results were normalized to the control group. Data are shown with mean±SE. ***P<0.001. (E) miR26a or miR26b suppressed 15-PGDH expression. CCLP1 or TFK-1 cells overexpressing miR26a or miR26b were transfected with anti-miR26 or scramble control. Total protein was analyzed 72h after transfection by Western blotting using 15-PGDH antibody. β-actin was measured as a reference gene. (F) miR26a or miR26b target 15-PGDH mRNA 3'UTR. CCLP1 and TFK-1 cells overexpressing miR26a or miR26b were transfected with 15-PGDH 3'UTR luciferase reporter vector or mutated construct. 72 hours after transfection, the cell lysates were obtained to measure luciferase activity. The results were normalized to control group and the data were presented as mean±SE. *P<0.05, ***P<0.001. (G) miR26a expression prevented ω-3 PUFA-induced 15-PGDH expression. CCLP1 and TFK-1 cells overexpressing miR26a were treated with or without 50 μM DHA for 12 h. Cellular

proteins were analyzed by Western blotting using 15-PGDH antibody (β-actin was measured as a reference gene).

Figure 17

A

3'AGgggAccaguCU_gAUGAACUC' miR4465
   II   I   II   II II I II
5'UCauuUuaaagGAgaUACUUGAA3' mutated 15-PGDH 3'UTR
         II   II I II II I
3'   guggaCUuaAUGAACUU5'miR1297

B
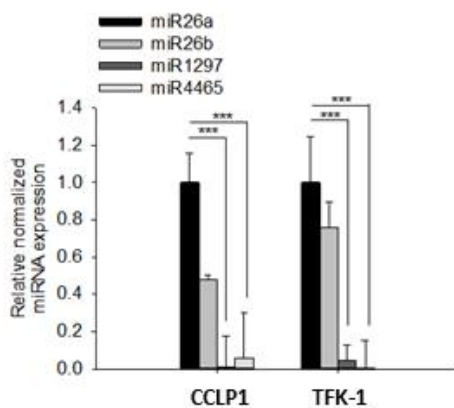
Figure 17. miRNAs that target 15-PGDH 3-UTR.

(A) Putative miR1297 and miR4465 binding sites in 3′-UTR of 15-PGDH mRNA.

(B) Relative expression levels of four 15-PGDH-targeting miRNAs in CCLP1 and TFK-

1 cells.

3. C-myc is implicated in v-3 PUFA-induced suppression of miR-26a/b

miR-26a/b are located in the introns of CTDSPs (carboxyterminal domain RNA polymerase II polypeptide A small phosphatase) gene family (illustrated in Figure. 18A; [114]). Given that the expression of miR-26a/b is reported to be concomitant with their host genes, we measured the mRNA level of CTDSPs (CTDSPL and CTDSP1) in cholangiocarcinoma cells treated with ω-3 PUFA. Our data showed that the ω-3 PUFA DHA suppressed the expression of both CTDSPL and CTDSP1, whereas the w-6 PUFA AA had no effect (Figure. 18B). The pattern of CTDSPL and CTDSP1 alterations appears to be similar to their intronic microRNAs, suggesting that miR-26a/b and their host genes are coregulated by w-6 PUFA in cholangiocarcinoma cells.

The expression of CTDSPs is well known to be associated with the transcription factor c-myc. Given that c-myc is a downstream gene of Wnt signaling [115, 116] and that ω-3 PUFA suppresses the Wnt pathway [117, 118], we sought to further examine whether c-myc might be implicated in ω-3 PUFA mediated suppression of CTDSPs/miR-26s. Our data showed that DHA treatment decreased c-myc along with reduction of CTDSPs/miR-26s (Figure. 18C and D). Importantly, DHA-induced reduction of CTDSPs/miR-26s was partially reversed by overexpression of c-myc (Figure. 18C and D). Chromatin immunoprecipitation (ChIP) assay showed that c-myc was associated with the promoters of the CTDSPL/miR-26a and CTDSP1/miR-26b gene clusters (Figure. 18E). These findings suggest that w-3 PUFA regulates the expression of miR-26a/b at least in part through c-myc.

Figure 18
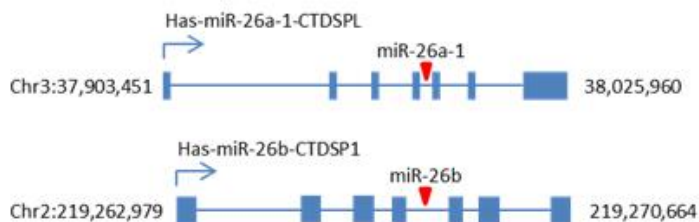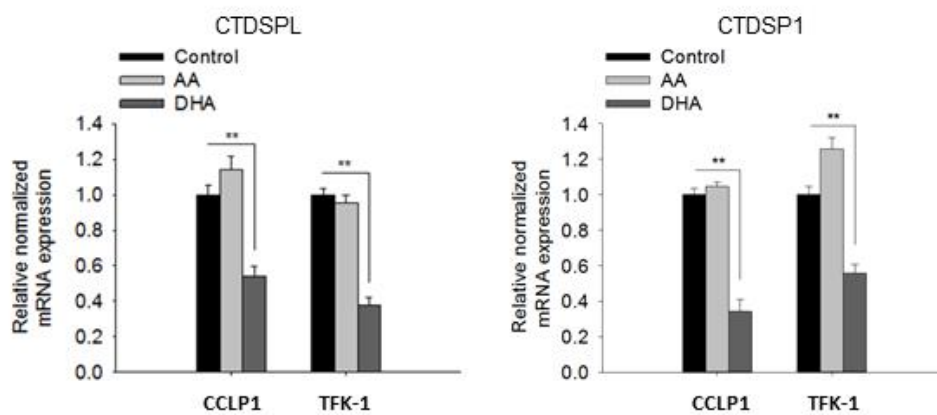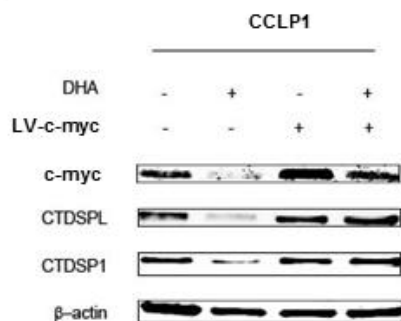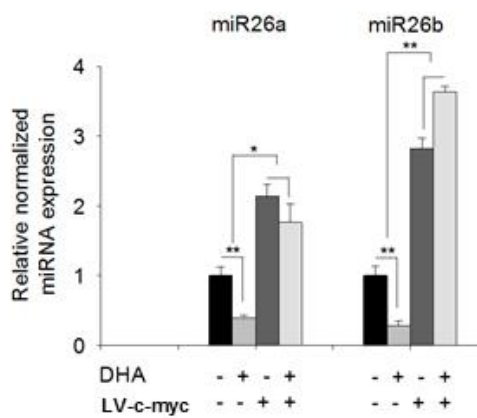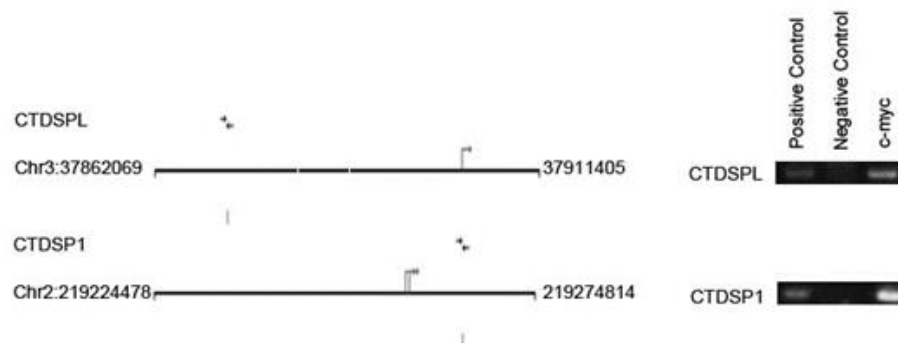
Figure 18: C-myc is implicated in ω-3 PUFA-induced suppression of miR26a/b.

(A) Schematic representation of gene map for miR26a/b and their host gene CTDSPL and CTDSP1; (B) DHA, but not AA, decreases the mRNA levels of miR26a/b host genes CTDSPL/CTDSP1 in cholangiocarcinoma cells. CCLP1 or TFK-1 cells were synchronized by serum deprivation, and then maintained in serum-free medium containing 50 μM DHA or AA for 12 h. CTDSPL or CTDSP1 mRNA was measured by real-time PCR. Results were normalized to control group; the data were shown with mean±SE. **P<0.01. (C) c-myc overexpression prevents DHA induced inhibition of CTDSPL and CTDSP1. CCLP1 cells infected with c-myc lentivirus or scramble control were maintained in serum free culture medium with or without 50 μM DHA for 12 h. Cellular proteins were analyzed by Western blotting with antibody against c-myc, CTDSPL and CTDSP1, respectively. β-actin was measured as a reference gene. (D) c-myc overexpression prevents DHA induced inhibition of miR26a or miR26b. CCLP1 cells infected with c-myc lentivirus or scramble control were treated with or without 50 μM DHA for 12 h. The levels of miR26a and miR26b were measured by real-time PCR. Results were normalized to the control group; data are shown with mean±SE. *P<0.05, **P<0.01; (E) c-myc binds to CTDSPL and CTDSP1 promoter region. Putative c-myc binding sites of CTDSPL and CTDSP1 promoter are shown. ChIP assay was performed by using antibody against c-myc to precipitate chromosome; antibody against Histone 3 was used as a positive control and Rabbit IgG as a negative control. Purified precipitating DNA was analyzed by PCR with primers amplifying c-myc binding regions in CTDSPL and CTDSP1 gene promoters.

4. Overexpression of miR-26a prevents Fat-1–induced inhibition of cholangiocarcinoma growth

To further determine the role of miR-26/15-PGDH in ω-3 PUFA-induced inhibition of cholangiocarcinoma cell growth, we evaluated the growth parameters of tumor cells overexpressing Fat1 and/or miR-26a. As shown in Figure 19A and B, overexpression of miR-26a abolished Fat-1–induced inhibition of CCLP1 cell growth and colony formation, in vitro. TUNEL assay showed that Fat-1–induced CCLP1 cell apoptosis was partially reversed by miR-26a overexpression (this result is consistent with our previous report that w-3 PUFAs inhibit cholangiocarcinoma predominantly through induction of apoptosis; [119]). Our further Western blotting analysis confirmed that miR-26a overexpression attenuated Fat-1–induced induction of 15-PGDH (Figure. 19C).

We then inoculated CCLP1 cells with or without Fat-1 and/or miR-26a overexpression subcutaneously into SCID mice to monitor tumor growth in vivo. Although Fat-1 expression inhibited xenograft tumor growth, overexpression of miR-26a enhanced tumor growth and offset the inhibitory effect of Fat-1 (Figure. 20A and B). Western blotting analysis using the recovered xenograft tumor tissues confirmed that miR-26a overexpression attenuated Fat-1–induced induction of 15-PGDH in vivo (Figure. 20C).

Figure 19

A
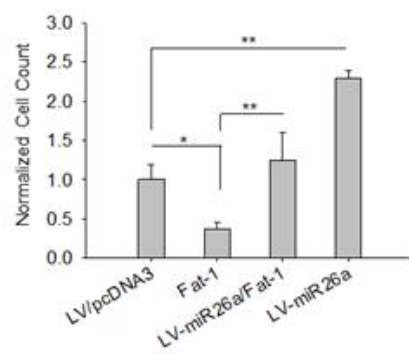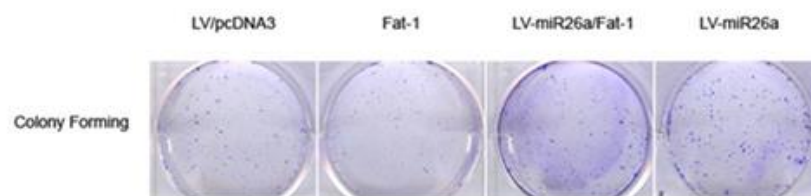
B
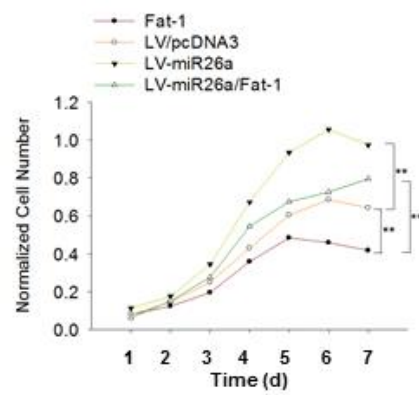
C
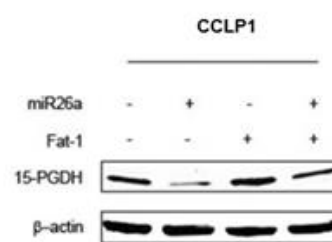
Figure 19: Overexpression of miR26a prevents Fat-1-induced inhibition of cholangiocarcinoma growth *in vitro*.

Different groups of CCLP1 cells (Fat-1 expression, miR26a overexpression, Fat-1/miR26a co-expression and control) were analyzed for cell proliferation by WST-1 assay and by colony formation assay. (A) Overexpression of Fat-1 inhibited CCLP1 colony forming ability; this effect was reversed by overexpression of miR-26a. Overexpression of miR26a alone was found to enhance CCLP1 colony formation efficiency. Representative results of three independent experiments were showed in upper panel. Quantified results were normalized to control group and presented as mean±SE in the lower panel; *P<0.05; **P<0.01; (B) Overexpression Fat-1 inhibited CCLP1 growth *in vitro*; this effect was reversed by miR26a overexpression. Overexpression miR26a alone significantly enhanced CCLP1 growth. The data are presented as mean±SE from 3 independent experiments. **P<0.01; (C) The levels of 15-PGDH protein in CCLP1 cells with Fat-1 overexpression, miR26a overexpression, Fat-1/miR26a co-expression, or control vector cells. Total protein was analyzed by Western blot with 15-PGDH antibody. β-actin were measured as a reference gene.

Figure 20
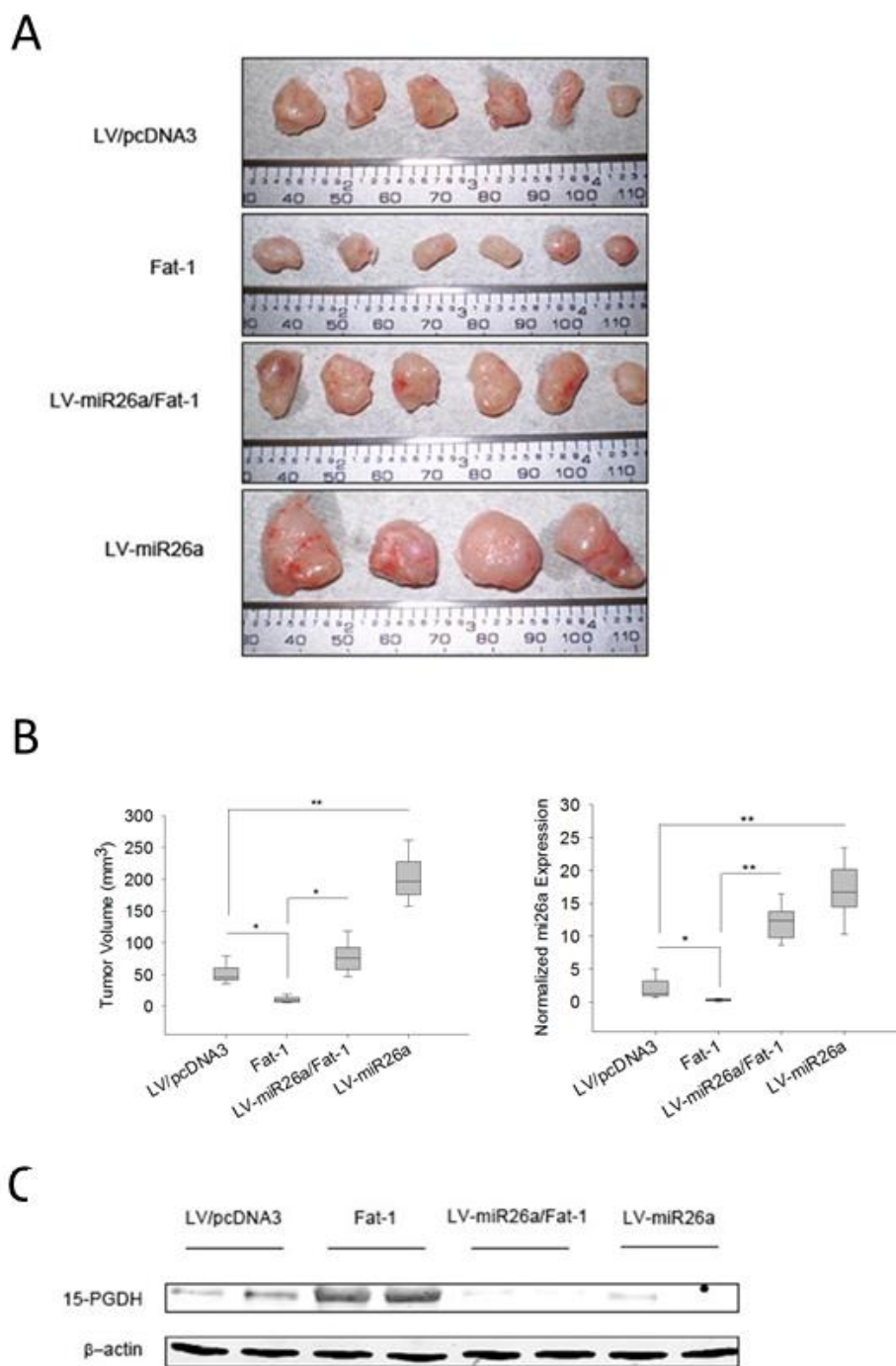
Figure 20: ω-3 PUFAs induce 15-PGDH and inhibit cholangiocarcinoma growth in vivo.

CCLP1 (with Fat-1 overexpression, miR26a overexpression, Fat-1/miR26a co-expression or control vector cells) were inoculated into SCID mice (n=6). Tumor growth was monitored and recovered 35 days later. Overexpression of Fat-1 inhibited tumor growth *in vivo*; this effect was reversed by overexpression of miR26a. Overexpression miR26a alone was found to enhance tumor growth *in vivo*. **(A)** Gross photograph of tumors recovered from SCID mice. **(B)** Bar graphs showing the average volume of recovered tumors and the average miR26a expression levels in the recovered tumors. The volume of tumor was calculated as described in the methods; the level of miR26a was measured by real-time PCR. Results were normalized to control group. Data was presented as mean mean±SE, *P<0.05, **P<0.01; **(C)** Representative Western blot for 15-PGDH in recovered tumor tissues. β-actin was measured as a reference gene.

5. Knockdown of 15-PGDH prevents v-3 PUFA-induced inhibition of cholangiocarcinoma growth

To further determine the role of 15-PGDH in w-3 PUFA induced inhibition of cholangiocarcinoma growth, we constructed cells with Fat-1 overexpressing plus 15-PGDH knockdown. By using an siRNA approach, we were able to satisfactorily reduce 15-PGDH protein in normal or Fat-1–expressed CCLP1 cells (Figure 21A). We observed that knockdown of 15-PGDH reversed Fat-1–induced inhibition of CCLP1 cell proliferation and colony formation, in vitro (Figure 21B and C). We next performed in vivo experiments to evaluate the effect of w-3 PUFAs and 15-PGDH on cholangiocarcinoma growth in SCID mice. We observed that administration of exogenous DHA to SCID mice significantly decreased tumor growth when the mice were inoculated with control vector tumor cells and that 15-PGDH knockdown reversed the DHA effect in vivo (Figure 22). These findings provide in vitro and in vivo evidence for an important role of 15-PGDH in w-3 PUFA induced inhibition of cholangiocarcinoma cell growth.

Figure 21
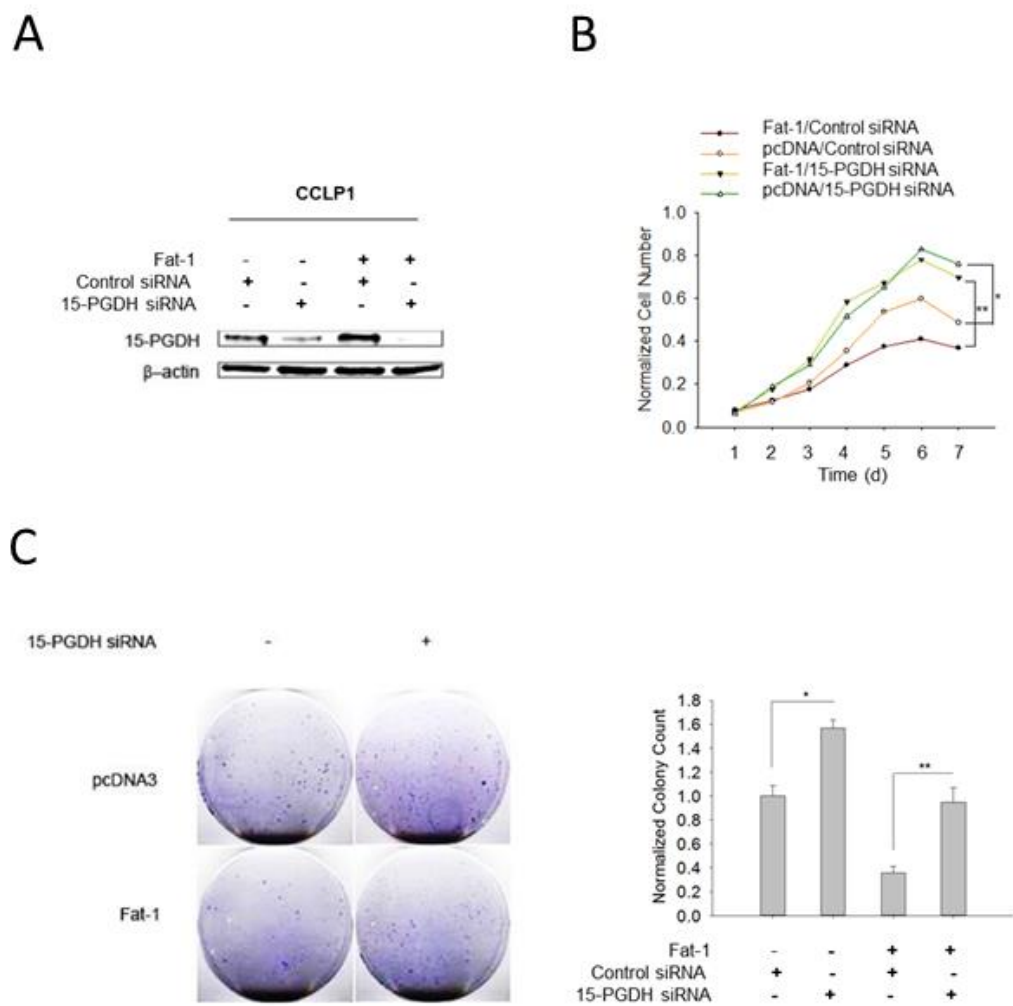
Figure 21: Knockdown of 15-PGDH prevents Fat-1-induced inhibition of cholangiocarcinoma growth.

Fat-1 overexpressing or control CCLP1 cells were transfected with 15-PGDH siRNA and the cells were evaluated for proliferation (WST-1) and colony formation. (A) The levels of 15-PGDH protein in cells with or without 15-PGDH knockdown. The cells were lysed 72 h after 15-PGDH siRNA transfection; total protein was analyzed by western blot with 15-PGDH antibody (β-actin was measured as a reference gene). (B) Knockdown 15-PGDH enhances CCLP1 cell growth and prevents Fat-1 induced inhibition of growth. The data are presented as mean±SE from 3 independent experiments. *$P<0.05$; **$P<0.01$; (C) Knockdown of 15-PGDH in CCLP1 cells prevents Fat-1 induced inhibition of colony formation. Representative of three independent experiments are showed in the left panel. Quantified results were normalized to vector control group and presented as mean±SE in the right panel; *$P<0.05$; **$P<0.01$.

Figure 22

A

Vector Control   15-PGDH KO

BSA Control

DHA
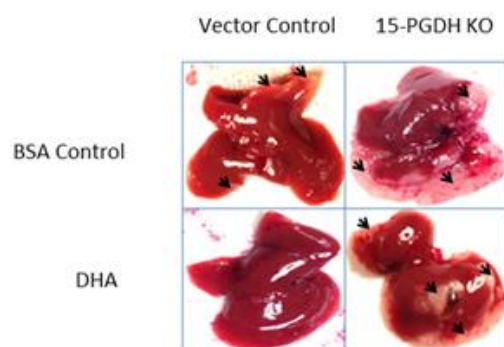
B
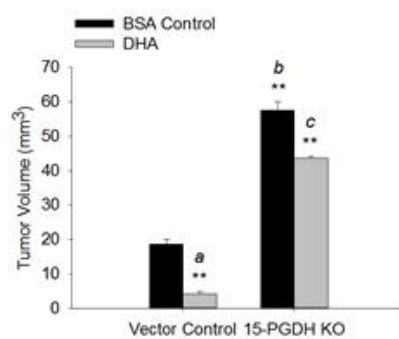
Figure 22. The effect of 15-PGDH and DHA on cholangiocarcinoma growth in vivo.

CCLP1 cells with or without 15-PGDH knockdown were inoculated into SCID mice via splenic injection and the animals were treated with DHA or BSA control as described in Materials and Methods. A, representative gross images of the liver from each group of mice. Arrowheads, areas of tumor growth. B, average tumor volume (**, P < 0.01; a, compared with the vector control group with BSA injection; b, compared with the vector control group with BSA injection; c, compared with the vector control group with BSA þ DHA injection).

6. Discussion

The current study provides the first evidence that ω-3 PUFAs up-regulate the expression of 15-PGDH by inhibiting miR26a and miR26b and that these effects contribute to ω-3 PUFA-induced inhibition of cholangiocarcinoma growth. Our findings support that ω-3 PUFA may be utilized as a non-toxic adjuvant therapeutic agent for the prevention and treatment of human cholangiocarcinoma. The significance of the study is further underscored by the fact that cholangiocarcinoma is a highly malignant human cancer currently with no effective prevention or treatment.

ω-3 PUFAs selectively inhibit cultured cholangiocarcinoma cells growth, but are significantly less toxic toward primary biliary epithelial cells [120]. This fact makes ω-3 PUFAs a potential non-toxic therapeutic agent for treatment of human cholangiocarcinoma. Several mechanisms for ω-3 PUFA as a cancer therapeutic agent have been documented [121]. A previous study from our group has shown that ω-3 PUFAs inhibit cholangiocarcinoma cell growth in part through inhibition of Wnt/beta-catenin and COX-2 signaling pathways [120]. The current study describes a separate novel mechanism, miR-26a/b-mediated regulation of 15-PGDH, in ω-3 PUFA-mediated inhibition of human cholangiocarcinoma. It is notable that 15-PGDH, a key enzyme that catalyzes PGE_2 oxidation, is an important tumor suppressor regulated by ω-3 PUFA. Our results show that ω-3 PUFA up-regulates 15-PGDH expression in cholangiocarcinoma cells and this effect contributes to inhibition of cholangiocarcinoma growth, in vitro and in vivo.

The mechanisms for 15-PGDH-mediated inhibition of cholangiocarcinoma growth include deactivation of PGE_2, a pro-inflammatory and pro-tumorigenic lipid mediator which is known to promote tumor growth, invasion and angiogenesis [73]. In parallel, 15-PGDH catalyzes the biotransformation of PGE_2 to 15-keto-PGE_2 which is known to activate peroxisome proliferator-activated receptor γ (PPARγ) and Smad2/3 leading to induction of TAp63 and inhibition of cholangiocarcinoma cell growth [12]. It is possible that all of these mechanisms may be implicated in ω-3 PUFA-induced inhibition of cholangiocarcinoma cell growth.

Our findings presented in the current study suggest that induction of 15-PGDH by ω-3 PUFA may represent an effective therapeutic target for CCA prevention and treatment. Since the cardiovascular side effect associated with COX-2 inhibitors is largely due to inhibition of the antithrombotic prostacyclin (PGI_2), induction or reaction of 15-PGDH is expected to block CCA growth without inhibiting PGI_2 and thus incurring no significant side effect. In this context, the results presented in this study are expected to have significant impact for future management of CCA.

Another novel aspect of the current study is the illustration of miR26a/b as a key factor linking ω-3 PUFA to 15-PGDH. We show that ω-3 PUFA inhibits the expression of miR26a/b, thus leading to 15-PGDH protein accumulation. Direct targeting of 15-PGDH by miR26a/b was demonstrated by the observations that miR26a/b inhibits 15-PGDH 3'UTR luciferase reporter activity and that miR26a/b overexpression prevents ω-3 PUFA-induced 15-PGDH protein accumulation. We note that knockdown of 15-PGDH did not reverse cholangiocarcinoma growth as potently as miR26a overexpression; this aspect may be explained by the facts that miR26s enhance Wnt/β-catenin signaling via

inhibiting GSK-3β and that GSK-3β is another target of ω-3 PUFA [12]. Thus, the data presented in the current study, along with our previous findings, suggest that there are two targets, 15-PGDH and GSK-3β, which can be regulated by ω-3 PUFA/miR26s in human cholangiocarcinoma cells. The interplay between PGE_2 and Wnt/β-catenin signaling pathways and their regulation by ω-3 PUFA are illustrated in Supplementary Figure S5.

While c-myc is a downstream oncogene of Wnt/β-catenin signaling, it is also the co-factor regulating the gene clusters formed by miR26a/b and their host CTDSPs genes. Our data presented in the current study suggest that ω-3 PUFA suppress miRNA26a and miRNA26b by inhibiting c-myc, through regulation of their host genes CTDSPs. The latter assertion is further supported by the ChIP assay showing that c-myc is associated with the promoters of the CTDSPL/miR26a and CTDSP1/miR26b gene clusters and by the observation that over-expression of c-myc prevents ω-3 PUFA-induced reduction of CTDSPs/miR26s.

In summary, the current study provides novel evidence for induction 15-PGDH by ω-3 PUFA via suppression of miR26s in human cholangiocarcinoma cells. Our findings further support the use of ω-3 PUFA as non-toxic adjuvant therapeutic agent for (the prevention and) treatment of human cholangiocarcinoma.

CONCLUSION

mPGES-1 is the terminal enzyme for the synthesis of PGE_2, which is a cytokine-inducible enzyme critically involved in PGE_2 mediated liver inflammation, tissue reparation and carcinogenesis. In first part of this study, we investigated the potential role of mPGES-1/PGE_2 in Fas-induced hepatocyte apoptosis and acute liver injury. We generated transgenic mice with targeted expression of mPGES-1 in the liver (mPGES-1 Tg); the transgenic mice were subjected to intraperitoneal injection of the Fas antibody Jo2. Our data showed that mPGES-1 overexpression prevents Fas-induced hepatocyte apoptosis and liver injury through activation of Akt and related signaling molecules. Consistent with these findings, we observed that inhibition of mPGES-1 or Akt restored the sensitivity of the mPGES-1 Tg mice to Jo2-induced liver injury. Our data support the anti-apoptotic role of PGE_2 mediated Akt activation in the liver which is important for protection against Fas-induced hepatocyte apoptosis.

15-PGDH is known to catalyze the oxidation of PGE_2, converting bioactive PGE_2 to its oxidized product, 15-keto-PGE_2 (a potential PPAR-γ ligand). Induction of 15-PGDH not only decreased PGE_2, but also raised the 15-keto-PGE_2 concentration. In the second part of this study, we developed liver specific 15-PGDH transgenic mice and the animals were subjected to LPS-induced liver inflammation/injury. We observed that the

15-PGDH transgenic mice were resistant to LPS-induced liver inflammation/injury. Mechanistically, our data showed that the 15-PGDH-derived 15-keto-PGE$_2$ from hepatocytes activated PPAR-γ in Kupffer cells and thus inhibited their ability to produce inflammatory cytokines and that this paracrine mechanism led to attenuation of necro-inflammatory response in the liver. Our results provide complementary evidence that PGE$_2$ promotes endotoxin induced liver inflammation and consequently tissue damage. In addition, we provide novel evidence that PGE$_2$ metabolites 15-keto-PGE$_2$ may have therapeutic benefits in treatment of inflammation-associated liver injury.

PGE2 is a pro-inflammatory and pro-tumorigenic lipid mediator that promotes liver tumorigenesis including cholangiocarcinoma growth in vitro and in vivo. Induction of 15-PGDH expression represents a new strategy for the prevention and treatment of PGE$_2$ dependent cholangiocarcinoma. In the third part of this study, we report that ω-3 PUFA (but not ω-6 PUFA) up-regulates the expression of 15-PGDH by inhibiting miR26a and miR26b in human cholangiocarcinoma cells. We show that 15-PGDH is a bona fide target of miR26a and miR26b. Our findings provide novel evidence for ω-3 PUFA-regulated miR26a/b and 15-PGDH cascade and support inhibiting PGE$_2$ as a therapeutic target for the prevention and treatment of human cholangiocarcinoma.

LIST OF REFERENCE

1.   Nakanishi, M. and D.W. Rosenberg, *Multifaceted roles of PGE2 in inflammation and cancer.* Semin Immunopathol, 2013. **35**(2): p. 123-37.

2.   Kalinski, P., *Regulation of immune responses by prostaglandin E2.* J Immunol, 2012. **188**(1): p. 21-8.

3.   Fujino, H., W. Xu, and J.W. Regan, *Prostaglandin E2 induced functional expression of early growth response factor-1 by EP4, but not EP2, prostanoid receptors via the phosphatidylinositol 3-kinase and extracellular signal-regulated kinases.* J Biol Chem, 2003. **278**(14): p. 12151-6.

4.   Fujino, H., K.A. West, and J.W. Regan, *Phosphorylation of glycogen synthase kinase-3 and stimulation of T-cell factor signaling following activation of EP2 and EP4 prostanoid receptors by prostaglandin E2.* J Biol Chem, 2002. **277**(4): p. 2614-9.

5.   Hata, A.N. and R.M. Breyer, *Pharmacology and signaling of prostaglandin receptors: multiple roles in inflammation and immune modulation.* Pharmacol Ther, 2004. **103**(2): p. 147-66.

6.   Nakanishi, M. and D.W. Rosenberg, *Roles of cPLA2alpha and arachidonic acid in cancer.* Biochim Biophys Acta, 2006. **1761**(11): p. 1335-43.

7.   Menter, D.G. and R.N. Dubois, *Prostaglandins in cancer cell adhesion, migration, and invasion.* Int J Cell Biol, 2012. **2012**: p. 723419.

8.   Wang, D. and R.N. Dubois, *Prostaglandins and cancer.* Gut, 2006. **55**(1): p. 115-22.

9.   Jakobsson, P.J., et al., *Identification of human prostaglandin E synthase: a microsomal, glutathione-dependent, inducible enzyme, constituting a potential novel drug target.* Proc Natl Acad Sci U S A, 1999. **96**(13): p. 7220-5.

10.   Murakami, M., et al., *Regulation of prostaglandin E2 biosynthesis by inducible membrane-associated prostaglandin E2 synthase that acts in concert with cyclooxygenase-2.* J Biol Chem, 2000. **275**(42): p. 32783-92.

11.   Lu, D., C. Han, and T. Wu, *15-PGDH inhibits hepatocellular carcinoma growth through 15-keto-PGE2/PPARgamma-mediated activation of p21WAF1/Cip1.* Oncogene, 2014. **33**(9): p. 1101-12.

12.   Lu, D., C. Han, and T. Wu, *15-hydroxyprostaglandin dehydrogenase-derived 15-keto-prostaglandin E2 inhibits cholangiocarcinoma cell growth through interaction with peroxisome proliferator-activated receptor-gamma, SMAD2/3, and TAP63 proteins.* J Biol Chem, 2013. **288**(27): p. 19484-502.

13.   Harmon, G.S., et al., *Pharmacological correction of a defect in PPAR-gamma signaling ameliorates disease severity in Cftr-deficient mice.* Nat Med, 2010. **16**(3): p. 313-8.

14.   Yu, Y.H., et al., *Prostaglandin reductase-3 negatively modulates adipogenesis through regulation of PPARgamma activity.* J Lipid Res, 2013. **54**(9): p. 2391-9.

15.   Wallace, J.L., *Prostaglandin biology in inflammatory bowel disease.* Gastroenterol Clin North Am, 2001. **30**(4): p. 971-80.

16.   Sheibanie, A.F., et al., *Prostaglandin E2 exacerbates collagen-induced arthritis in mice through the inflammatory interleukin-23/interleukin-17 axis.* Arthritis Rheum, 2007. **56**(8): p. 2608-19.

17.   Sheibanie, A.F., et al., *The proinflammatory effect of prostaglandin E2 in experimental inflammatory bowel disease is mediated through the IL-23-->IL-17 axis.* J Immunol, 2007. **178**(12): p. 8138-47.

18.   Muthuswamy, R., et al., *PGE(2) transiently enhances DC expression of CCR7 but inhibits the ability of DCs to produce CCL19 and attract naive T cells.* Blood, 2010. **116**(9): p. 1454-9.

19.   Joshi, P.C., et al., *Prostaglandin E2 suppressed IL-15-mediated human NK cell function through down-regulation of common gamma-chain.* J Immunol, 2001. **166**(2): p. 885-91.

20.   Quatromoni, J.G. and E. Eruslanov, *Tumor-associated macrophages: function, phenotype, and link to prognosis in human lung cancer.* Am J Transl Res, 2012. **4**(4): p. 376-89.

21.   Zhu, Z., et al., *Prostaglandin E2 promotes endothelial differentiation from bone marrow-derived cells through AMPK activation.* PLoS One, 2011. **6**(8): p. e23554.

22.   Harding, P. and M.C. LaPointe, *Prostaglandin E2 increases cardiac fibroblast proliferation and increases cyclin D expression via EP1 receptor.* Prostaglandins Leukot Essent Fatty Acids, 2011. **84**(5-6): p. 147-52.

23.   Buchanan, F.G., et al., *Prostaglandin E2 regulates cell migration via the intracellular activation of the epidermal growth factor receptor.* J Biol Chem, 2003. **278**(37): p. 35451-7.

24.   Fukunaga, K., et al., *Cyclooxygenase 2 plays a pivotal role in the resolution of acute lung injury.* J Immunol, 2005. **174**(8): p. 5033-9.

25.   Zhang, Y., et al., *TISSUE REGENERATION. Inhibition of the prostaglandin-degrading enzyme 15-PGDH potentiates tissue regeneration.* Science, 2015. **348**(6240): p. aaa2340.

26.   Hoggatt, J., et al., *Prostaglandin E2 enhances hematopoietic stem cell homing, survival, and proliferation.* Blood, 2009. **113**(22): p. 5444-55.

27. Eberhart, C.E., et al., *Up-regulation of cyclooxygenase 2 gene expression in human colorectal adenomas and adenocarcinomas.* Gastroenterology, 1994. **107**(4): p. 1183-8.

28. Kargman, S.L., et al., *Expression of prostaglandin G/H synthase-1 and -2 protein in human colon cancer.* Cancer Res, 1995. **55**(12): p. 2556-9.

29. Odeh, M., *Aspirin and risk of fatal colon cancer.* Postgrad Med J, 1993. **69**(809): p. 242.

30. Sinicrope, F.A. and S. Gill, *Role of cyclooxygenase-2 in colorectal cancer.* Cancer Metastasis Rev, 2004. **23**(1-2): p. 63-75.

31. Hong, K.H., et al., *Deletion of cytosolic phospholipase A(2) suppresses Apc(Min)-induced tumorigenesis.* Proc Natl Acad Sci U S A, 2001. **98**(7): p. 3935-9.

32. Chulada, P.C., et al., *Genetic disruption of Ptgs-1, as well as Ptgs-2, reduces intestinal tumorigenesis in Min mice.* Cancer Res, 2000. **60**(17): p. 4705-8.

33. Nakanishi, M., et al., *Genetic deletion of mPGES-1 suppresses intestinal tumorigenesis.* Cancer Res, 2008. **68**(9): p. 3251-9.

34. Chen, E.P. and E.M. Smyth, *COX-2 and PGE2-dependent immunomodulation in breast cancer.* Prostaglandins Other Lipid Mediat, 2011. **96**(1-4): p. 14-20.

35. Oshima, H., et al., *Hyperplastic gastric tumors induced by activated macrophages in COX-2/mPGES-1 transgenic mice.* EMBO J, 2004. **23**(7): p. 1669-78.

36.   Sheng, H., et al., *Modulation of apoptosis and Bcl-2 expression by prostaglandin E2 in human colon cancer cells.* Cancer Res, 1998. **58**(2): p. 362-6.

37.   Tsujii, M. and R.N. DuBois, *Alterations in cellular adhesion and apoptosis in epithelial cells overexpressing prostaglandin endoperoxide synthase 2.* Cell, 1995. **83**(3): p. 493-501.

38.   Sheng, H., et al., *Prostaglandin E2 increases growth and motility of colorectal carcinoma cells.* J Biol Chem, 2001. **276**(21): p. 18075-81.

39.   Tessner, T.G., et al., *Prostaglandin E2 reduces radiation-induced epithelial apoptosis through a mechanism involving AKT activation and bax translocation.* J Clin Invest, 2004. **114**(11): p. 1676-85.

40.   Leone, V., et al., *PGE2 inhibits apoptosis in human adenocarcinoma Caco-2 cell line through Ras-PI3K association and cAMP-dependent kinase A activation.* Am J Physiol Gastrointest Liver Physiol, 2007. **293**(4): p. G673-81.

41.   Pai, R., et al., *Prostaglandin E2 transactivates EGF receptor: a novel mechanism for promoting colon cancer growth and gastrointestinal hypertrophy.* Nat Med, 2002. **8**(3): p. 289-93.

42.   van de Wetering, M., et al., *The beta-catenin/TCF-4 complex imposes a crypt progenitor phenotype on colorectal cancer cells.* Cell, 2002. **111**(2): p. 241-50.

43.   Castellone, M.D., et al., *Prostaglandin E2 promotes colon cancer cell growth through a Gs-axin-beta-catenin signaling axis.* Science, 2005. **310**(5753): p. 1504-10.

44.   North, T.E., et al., *Prostaglandin E2 regulates vertebrate haematopoietic stem cell homeostasis.* Nature, 2007. **447**(7147): p. 1007-11.

45.   Tsujii, M., et al., *Cyclooxygenase regulates angiogenesis induced by colon cancer cells.* Cell, 1998. **93**(5): p. 705-16.

46.   Jones, M.K., et al., *Inhibition of angiogenesis by nonsteroidal anti-inflammatory drugs: insight into mechanisms and implications for cancer growth and ulcer healing.* Nat Med, 1999. **5**(12): p. 1418-23.

47.   Wang, D., et al., *CXCL1 induced by prostaglandin E2 promotes angiogenesis in colorectal cancer.* J Exp Med, 2006. **203**(4): p. 941-51.

48.   Dormond, O., et al., *NSAIDs inhibit alpha V beta 3 integrin-mediated and Cdc42/Rac-dependent endothelial-cell spreading, migration and angiogenesis.* Nat Med, 2001. **7**(9): p. 1041-7.

49.   Fenwick, S.W., et al., *The effect of the selective cyclooxygenase-2 inhibitor rofecoxib on human colorectal cancer liver metastases.* Gastroenterology, 2003. **125**(3): p. 716-29.

50. Tsujii, M., S. Kawano, and R.N. DuBois, *Cyclooxygenase-2 expression in human colon cancer cells increases metastatic potential.* Proc Natl Acad Sci U S A, 1997. **94**(7): p. 3336-40.

51. Pai, R., et al., *Prostaglandins promote colon cancer cell invasion; signaling by cross-talk between two distinct growth factor receptors.* FASEB J, 2003. **17**(12): p. 1640-7.

52. Gupta, G.P., et al., *Mediators of vascular remodelling co-opted for sequential steps in lung metastasis.* Nature, 2007. **446**(7137): p. 765-70.

53. Wernze, H., G. Muller, and M. Goerig, *Relationship between urinary prostaglandin (PGE2 and PGF2 alpha) and sodium excretion in various stages of chronic liver disease.* Adv Prostaglandin Thromboxane Res, 1980. **7**: p. 1089-96.

54. Liaskou, E., D.V. Wilson, and Y.H. Oo, *Innate immune cells in liver inflammation.* Mediators Inflamm, 2012. **2012**: p. 949157.

55. Renz, H., et al., *Release of tumor necrosis factor-alpha from macrophages. Enhancement and suppression are dose-dependently regulated by prostaglandin E2 and cyclic nucleotides.* J Immunol, 1988. **141**(7): p. 2388-93.

56. Olaso, E., et al., *Proangiogenic role of tumor-activated hepatic stellate cells in experimental melanoma metastasis.* Hepatology, 2003. **37**(3): p. 674-85.

57.   Li, G., et al., *Cyclooxygenase-2 prevents fas-induced liver injury through up-regulation of epidermal growth factor receptor.* Hepatology, 2009. **50**(3): p. 834-43.

58.   Tolba, R.H., et al., *Role of preferential cyclooxygenase-2 inhibition by meloxicam in ischemia/reperfusion injury of the rat liver.* Eur Surg Res, 2014. **53**(1-4): p. 11-24.

59.   Bhave, V.S., et al., *Secretory phospholipase A2 mediates progression of acute liver injury in the absence of sufficient cyclooxygenase-2.* Toxicol Appl Pharmacol, 2008. **228**(2): p. 225-38.

60.   Reilly, T.P., et al., *A protective role for cyclooxygenase-2 in drug-induced liver injury in mice.* Chem Res Toxicol, 2001. **14**(12): p. 1620-8.

61.   Turini, M.E. and R.N. DuBois, *Cyclooxygenase-2: a therapeutic target.* Annu Rev Med, 2002. **53**: p. 35-57.

62.   Martin-Sanz, P., et al., *Expression of cyclooxygenase-2 in foetal rat hepatocytes stimulated with lipopolysaccharide and pro-inflammatory cytokines.* Br J Pharmacol, 1998. **125**(6): p. 1313-9.

63.   Obermajer, N., et al., *Positive feedback between PGE2 and COX2 redirects the differentiation of human dendritic cells toward stable myeloid-derived suppressor cells.* Blood, 2011. **118**(20): p. 5498-505.

64.   Han, C., et al., *Transgenic expression of cyclooxygenase-2 in hepatocytes accelerates endotoxin-induced acute liver failure.* J Immunol, 2008. **181**(11): p. 8027-35.

65.   Takano, M., et al., *Prostaglandin E2 protects against liver injury after Escherichia coli infection but hampers the resolution of the infection in mice.* J Immunol, 1998. **161**(6): p. 3019-25.

66.   Okamoto, T., et al., *Immunological tolerance in a mouse model of immune-mediated liver injury induced by 16,16 dimethyl PGE2 and PGE2-containing nanoscale hydrogels.* Biomaterials, 2011. **32**(21): p. 4925-35.

67.   Casado, M., et al., *Protection against Fas-induced liver apoptosis in transgenic mice expressing cyclooxygenase 2 in hepatocytes.* Hepatology, 2007. **45**(3): p. 631-8.

68.   Yu, J., et al., *Elucidation of the role of COX-2 in liver fibrogenesis using transgenic mice.* Biochem Biophys Res Commun, 2008. **372**(4): p. 571-7.

69.   Casado, M., et al., *Contribution of cyclooxygenase 2 to liver regeneration after partial hepatectomy.* FASEB J, 2001. **15**(11): p. 2016-8.

70.   Martin-Sanz, P., et al., *COX-2 in liver, from regeneration to hepatocarcinogenesis: what we have learned from animal models?* World J Gastroenterol, 2010. **16**(12): p. 1430-5.

71.   Kumar, M., X. Zhao, and X.W. Wang, *Molecular carcinogenesis of hepatocellular carcinoma and intrahepatic cholangiocarcinoma: one step closer to personalized medicine?* Cell Biosci, 2011. **1**(1): p. 5.

72.   Wu, T., *Cyclooxygenase-2 in hepatocellular carcinoma.* Cancer Treat Rev, 2006. **32**(1): p. 28-44.

73.   Wu, T., *Cyclooxygenase-2 and prostaglandin signaling in cholangiocarcinoma.* Biochim Biophys Acta, 2005. **1755**(2): p. 135-50.

74.   Koga, H., et al., *Expression of cyclooxygenase-2 in human hepatocellular carcinoma: relevance to tumor dedifferentiation.* Hepatology, 1999. **29**(3): p. 688-96.

75.   Shiota, G., et al., *Cyclooxygenase-2 expression in hepatocellular carcinoma.* Hepatogastroenterology, 1999. **46**(25): p. 407-12.

76.   Bae, S.H., et al., *Expression of cyclooxygenase-2 (COX-2) in hepatocellular carcinoma and growth inhibition of hepatoma cell lines by a COX-2 inhibitor, NS-398.* Clin Cancer Res, 2001. **7**(5): p. 1410-8.

77.   Qiu, D.K., et al., *Significance of cyclooxygenase-2 expression in human primary hepatocellular carcinoma.* World J Gastroenterol, 2002. **8**(5): p. 815-7.

78.   Leng, J., et al., *Cyclooxygenase-2 promotes hepatocellular carcinoma cell growth through Akt activation: evidence for Akt inhibition in celecoxib-induced apoptosis.* Hepatology, 2003. **38**(3): p. 756-68.

79.   Mayoral, R., et al., *Prostaglandin E2 promotes migration and adhesion in hepatocellular carcinoma cells.* Carcinogenesis, 2005. **26**(4): p. 753-61.

80.   Cheng, A.S., et al., *Cyclooxygenase-2 pathway correlates with vascular endothelial growth factor expression and tumor angiogenesis in hepatitis B virus-associated hepatocellular carcinoma.* Int J Oncol, 2004. **24**(4): p. 853-60.

81.   Gupta, C., M. Banks, and H. Shinozuka, *Elevated levels of prostaglandin E2 in the liver of rats fed a choline deficient diet: possible involvement in liver tumor promotion.* Cancer Lett, 1989. **46**(2): p. 129-35.

82.   Tanaka, T., et al., *Inhibitory effect of the non-steroidal anti-inflammatory drugs, indomethacin and piroxicam on 2-acetylaminofluorene-induced hepatocarcinogenesis in male ACI/N rats.* Cancer Lett, 1993. **68**(2-3): p. 111-8.

83.   Denda, A., et al., *Possible involvement of arachidonic acid metabolism in phenobarbital promotion of hepatocarcinogenesis.* Carcinogenesis, 1989. **10**(10): p. 1929-35.

84.   Takii, Y., et al., *Expression of microsomal prostaglandin E synthase-1 in human hepatocelluar carcinoma.* Liver Int, 2007. **27**(7): p. 989-96.

85.   Lu, D., C. Han, and T. Wu, *Microsomal prostaglandin E synthase-1 promotes hepatocarcinogenesis through activation of a novel EGR1/beta-catenin signaling axis.* Oncogene, 2012. **31**(7): p. 842-57.

86. Takasu, S., et al., *Roles of cyclooxygenase-2 and microsomal prostaglandin E synthase-1 expression and beta-catenin activation in gastric carcinogenesis in N-methyl-N-nitrosourea-treated K19-C2mE transgenic mice.* Cancer Sci, 2008. **99**(12): p. 2356-64.

87. Hayashi, N., et al., *Differential expression of cyclooxygenase-2 (COX-2) in human bile duct epithelial cells and bile duct neoplasm.* Hepatology, 2001. **34**(4 Pt 1): p. 638-50.

88. Endo, K., et al., *ERBB-2 overexpression and cyclooxygenase-2 up-regulation in human cholangiocarcinoma and risk conditions.* Hepatology, 2002. **36**(2): p. 439-50.

89. Chariyalertsak, S., et al., *Aberrant cyclooxygenase isozyme expression in human intrahepatic cholangiocarcinoma.* Gut, 2001. **48**(1): p. 80-6.

90. Tsubouchi, H., *Sustained activation of epidermal growth factor receptor in cholangiocarcinoma: a potent therapeutic target?* J Hepatol, 2004. **41**(5): p. 859-61.

91. Yoon, J.H., et al., *Enhanced epidermal growth factor receptor activation in human cholangiocarcinoma cells.* J Hepatol, 2004. **41**(5): p. 808-14.

92. Wojcik, M., et al., *Immunodetection of cyclooxygenase-2 (COX-2) is restricted to tissue macrophages in normal rat liver and to recruited mononuclear phagocytes*

in liver injury and cholangiocarcinoma. Histochem Cell Biol, 2012. **137**(2): p. 217-33.

93.   Wu, G.S., et al., *Bile from a patient with anomalous pancreaticobiliary ductal union promotes the proliferation of human cholangiocarcinoma cells via COX-2 pathway.* World J Gastroenterol, 2003. **9**(5): p. 1094-7.

94.   Nzeako, U.C., et al., *COX-2 inhibits Fas-mediated apoptosis in cholangiocarcinoma cells.* Hepatology, 2002. **35**(3): p. 552-9.

95.   Wu, T., et al., *Involvement of 85-kd cytosolic phospholipase A(2) and cyclooxygenase-2 in the proliferation of human cholangiocarcinoma cells.* Hepatology, 2002. **36**(2): p. 363-73.

96.   Lu, D., C. Han, and T. Wu, *Microsomal prostaglandin E synthase-1 inhibits PTEN and promotes experimental cholangiocarcinogenesis and tumor progression.* Gastroenterology, 2011. **140**(7): p. 2084-94.

97.   Liu, D., et al., *Nuclear import of proinflammatory transcription factors is required for massive liver apoptosis induced by bacterial lipopolysaccharide.* J Biol Chem, 2004. **279**(46): p. 48434-42.

98.   Dajani, O.F., et al., *Prostaglandin E2 upregulates EGF-stimulated signaling in mitogenic pathways involving Akt and ERK in hepatocytes.* J Cell Physiol, 2008. **214**(2): p. 371-80.

99.   Refsnes, M., et al., *Stimulation of hepatocyte DNA synthesis by prostaglandin E2 and prostaglandin F2 alpha: additivity with the effect of norepinephrine, and synergism with epidermal growth factor.* J Cell Physiol, 1994. **159**(1): p. 35-40.

100.   Hashimoto, N., et al., *Prostaglandins induce proliferation of rat hepatocytes through a prostaglandin E2 receptor EP3 subtype.* Am J Physiol, 1997. **272**(3 Pt 1): p. G597-604.

101.   Kimura, M., S. Osumi, and M. Ogihara, *Prostaglandin E(2) (EP(1)) receptor agonist-induced DNA synthesis and proliferation in primary cultures of adult rat hepatocytes: the involvement of TGF-alpha.* Endocrinology, 2001. **142**(10): p. 4428-40.

102.   North, T.E., et al., *PGE2-regulated wnt signaling and N-acetylcysteine are synergistically hepatoprotective in zebrafish acetaminophen injury.* Proc Natl Acad Sci U S A, 2010. **107**(40): p. 17315-20.

103.   Rincon-Sanchez, A.R., et al., *PGE2 alleviates kidney and liver damage, decreases plasma renin activity and acute phase response in cirrhotic rats with acute liver damage.* Exp Toxicol Pathol, 2005. **56**(4-5): p. 291-303.

104.   Mayoral, R., et al., *Constitutive expression of cyclo-oxygenase 2 transgene in hepatocytes protects against liver injury.* Biochem J, 2008. **416**(3): p. 337-46.

105. Nowak, M., et al., *LPS-induced liver injury in D-galactosamine-sensitized mice requires secreted TNF-alpha and the TNF-p55 receptor.* Am J Physiol Regul Integr Comp Physiol, 2000. **278**(5): p. R1202-9.

106. Schwabe, R.F. and D.A. Brenner, *Mechanisms of Liver Injury. I. TNF-alpha-induced liver injury: role of IKK, JNK, and ROS pathways.* Am J Physiol Gastrointest Liver Physiol, 2006. **290**(4): p. G583-9.

107. Zimmermann, H.W., C. Trautwein, and F. Tacke, *Functional role of monocytes and macrophages for the inflammatory response in acute liver injury.* Front Physiol, 2012. **3**: p. 56.

108. Galanos, C., M.A. Freudenberg, and W. Reutter, *Galactosamine-induced sensitization to the lethal effects of endotoxin.* Proc Natl Acad Sci U S A, 1979. **76**(11): p. 5939-43.

109. Ogawa, Y., et al., *Peroxisome Proliferator-Activated Receptor Gamma Exacerbates Concanavalin A-Induced Liver Injury via Suppressing the Translocation of NF-kappaB into the Nucleus.* PPAR Res, 2012. **2012**: p. 940384.

110. Pascual, G., et al., *A SUMOylation-dependent pathway mediates transrepression of inflammatory response genes by PPAR-gamma.* Nature, 2005. **437**(7059): p. 759-63.

111. Pascual, G. and C.K. Glass, *Nuclear receptors versus inflammation: mechanisms of transrepression.* Trends Endocrinol Metab, 2006. **17**(8): p. 321-7.

112. FitzGerald, G.A., *BIOMEDICINE. Bringing PGE(2) in from the cold.* Science, 2015. **348**(6240): p. 1208-9.

113. Kang, J.X., et al., *Transgenic mice: fat-1 mice convert n-6 to n-3 fatty acids.* Nature, 2004. **427**(6974): p. 504.

114. Zhu, Y., et al., *MicroRNA-26a/b and their host genes cooperate to inhibit the G1/S transition by activating the pRb protein.* Nucleic Acids Res, 2012. **40**(10): p. 4615-25.

115. Han, J., A.M. Denli, and F.H. Gage, *The enemy within: intronic miR-26b represses its host gene, ctdsp2, to regulate neurogenesis.* Genes Dev, 2012. **26**(1): p. 6-10.

116. Frenzel, A., J. Loven, and M.A. Henriksson, *Targeting MYC-Regulated miRNAs to Combat Cancer.* Genes Cancer, 2010. **1**(6): p. 660-7.

117. Sander, S., L. Bullinger, and T. Wirth, *Repressing the repressor: a new mode of MYC action in lymphomagenesis.* Cell Cycle, 2009. **8**(4): p. 556-9.

118. Song, K.S., et al., *Omega-3-polyunsaturated fatty acids suppress pancreatic cancer cell growth in vitro and in vivo via downregulation of Wnt/Beta-catenin signaling.* Pancreatology, 2011. **11**(6): p. 574-84.

119. Han, C., et al., *Transforming growth factor-beta (TGF-beta) activates cytosolic phospholipase A2alpha (cPLA2alpha)-mediated prostaglandin E2 (PGE)2/EP1 and peroxisome proliferator-activated receptor-gamma (PPAR-gamma)/Smad*

signaling pathways in human liver cancer cells. A novel mechanism for subversion of TGF-beta-induced mitoinhibition. J Biol Chem, 2004. **279**(43): p. 44344-54.

120. Lim, K., et al., *Cyclooxygenase-2-derived prostaglandin E2 activates beta-catenin in human cholangiocarcinoma cells: evidence for inhibition of these signaling pathways by omega 3 polyunsaturated fatty acids.* Cancer Res, 2008. **68**(2): p. 553-60.

121. Stephenson, J.A., et al., *The multifaceted effects of omega-3 polyunsaturated Fatty acids on the hallmarks of cancer.* J Lipids, 2013. **2013**: p. 261247.

LIST OF ABBREVIATIONS

PGE$_2$ Prostaglandin E2

COX-1/2   Cyclooxygenase 1/2

mPGES-1/2   Microsomal prostaglandin E synthase 1/2

Akt   Protein kinase B

HCC   Hepatocellular carcinoma

ω-3 PUFA   Omega-3 polyunsaturated fatty acid

EP 1-4   E-prostanoid receptors 1-4

GPCR   G-protein coupled receptors

cAMP   Cyclic AMP

PI3K   Phosphoinositide 3-kinase

ERK   Extracellular-signal-regulated kinases

GSK3   Glycogen synthase kinase 3

β-catenin   Catenin beta-1

AA	Arachidonic acid
$cPLA_2\alpha$	Cytosolic phospholipase A2 alpha
MAPK	Mitogen-activated protein kinase
cPGES	Cytosolic PGE synthase
15-PGDH	15-hydroxyprostaglandin dehydrogenase
PPAR-γ	Peroxisome proliferator-activated receptor γ
IL17	Interleukin 17
CCL19	Chemokine (C-C motif) ligand 19
IL2	Interleukin 2
VEGF	Vascular endothelial growth factor
AMPK	AMP-activated protein kinase
JNK	c-Jun N-terminal kinases
EGFR	Epidermal growth factor receptor
$dmPGE_2$	16, 16-dimethyl-PGE2
DMBA	Dimethylbenzanthracene
CXCL1	Chemokine (C-X-C motif) ligand 1
TNF-α	Tumor necrosis factor-α

IL-1β   Interleukin 1 beta

IFN-γ   interferon-γ

BIOGRAPHY

Lu Yao was born on November 25th, 1985 in Tongchuan, Shaanxi, China. After graduated from Beijing Forestry University, Beijing, China with B.S. in Biological Science in June 2007, he attended Wuhan Institute of Virology, Chinese Academy of Science, Wuhan, Hubei, China, and received M.S. degree in Biochemistry and Molecular Biology in June 2010. In August 2010, He was enrolled in the graduate program in Biomedical Science, School of Medicine, Tulane University, New Orleans, LA, USA. There, He carried dissertation study on effect of PGs signaling in liver inflammation and carcinogenesis under supervision of Dr. Tong Wu and Dr. Chang Han. He finished his graduation study and received the degree of Ph.D. in Biomedical Science in December, 2015.